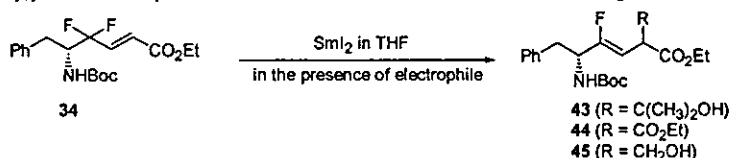


FIGURE 5. A plausible explanation for reversal of the stereochemical outcome with an imine derived from phenylacetaldehyde.

TABLE 3. Reduction of γ,γ -Difluoro- α,β -enoate with SmI_2 in the Presence of Electrophiles



entry	electrophile (equiv)	reagent (equiv, solvent)	condition	products ^a (isolated yield %)
1	BzIbR (3 equiv)	SmI_2 (6 equiv, THF)	0 °C, 60 min	<i>b</i>
2	CH_3COCH_3 (3 equiv)	SmI_2 (3 equiv, THF)	0 °C, 60 min	43 (82)
3	$(\text{EtOCO})_2\text{O}$ (5 equiv)	SmI_2 (6 equiv, THF)	0 °C, 60 min	44 (76)
4	HCHO (6 equiv) ^c	SmI_2 (3 equiv, THF)	0 °C, 60 min	45 (65)

^a Combined yield of diastereomers except for 44. ^b Unidentified products were formed. ^c Formaldehyde complex was prepared from *s*-trioxane (2 equiv), 2,6-diphenylphenol (12 equiv), and Me_3Al (6 equiv) in CH_2Cl_2 -hexane.

tion of several α -functionalized isosteres because the hydroxymethyl group can be easily converted to other functional groups. For such purposes, trapping of the dienolates with formaldehyde may be suitable; however, addition of commercially available formalin to the SmI_2 -mediated reduction resulted in failure to furnish Xaa-Gly-type isosteres. This was due to the predominant quenching with H_2O derived from the formalin solution. Yamamoto et al. reported that formaldehyde can be generated under aprotic conditions by treatment of readily available *s*-trioxane with methylaluminum bis-(2,6-diphenylphenoxide) (MAPH) to stabilize formaldehyde as a MAPH complex.⁴¹ The resulting complex is useful as a stable source of reactive formaldehyde in aprotic media for reactions with a variety of nucleophiles such as enolates and olefins. This work prompted us to use the formaldehyde-MAPH complex as a trapping reagent for dienolates derived from the SmI_2 -mediated reduction of **34**. Reaction with SmI_2 (3 equiv) in THF at 0 °C for 60 min of a mixture of **34** and the formaldehyde-MAPH complex (6 equiv), prepared as CH_2Cl_2 -hexane solution, gave a diastereomeric mixture of α -hydroxymethyl fluoroalkene isosteres (D-Phe- ψ [(*Z*)-CF=CH]-L/D-Ser) **45** in 65% isolated yield (Table 3, entry 4). As with

the enoate **34**, essentially no stereoselectivity was noted for these coupling reactions with either acetone or formaldehyde. It does not appear that the distal substituent on the δ -carbon has any stereodirecting effect with respect to the incoming electrophile. Enzyme-catalyzed enantioselective hydrolysis of esters is an attractive means to obtain chiral amino acid derivatives. However, attempted selective hydrolysis of the diastereomeric mixture **45** met with failure.

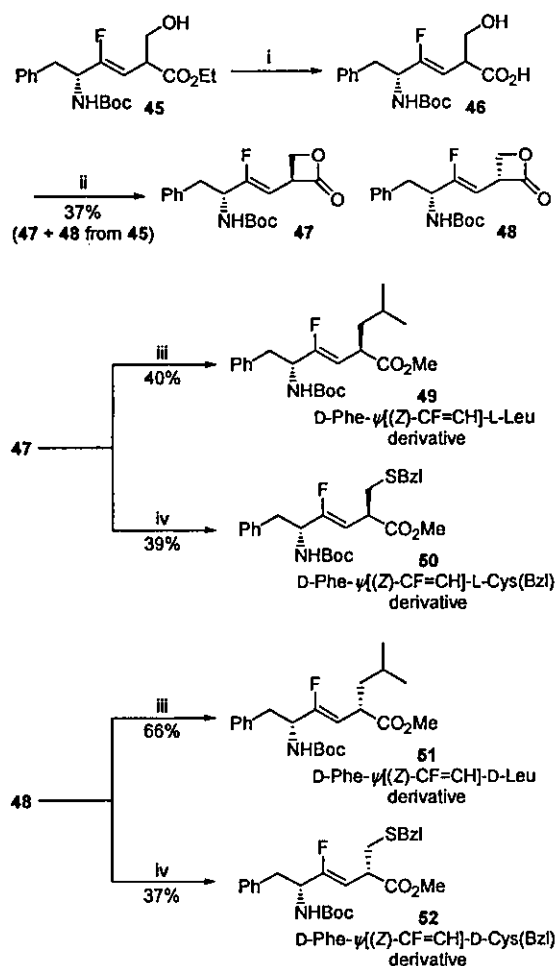
To transform the hydroxymethyl group to another side chain functionality, the Phe-Ser-type isostere **45** was subjected to saponification followed by intramolecular Mitsunobu reaction to afford β -lactone derivatives **47** and **48**, which were susceptible to soft nucleophiles⁴² (Scheme 3). Fortunately, at this stage, diastereomeric β -lactones **47** and **48** were easily separable by flash chromatography on silica gel. Reaction of β -lactone derivatives derived from protected serine with a variety of soft nucleophiles such as thiols and organocopper reagents has been reported to provide access to various *N*-protected amino acids that result from alkyl-oxygen cleavage.⁴² Treatment of each purified lactone **47** and **48** with isopropyl Grignard reagent in the presence of $\text{CuBr}\cdot\text{Me}_2\text{S}$ in THF, followed by TMSCHN_2 treatment,⁴³ proceeded with cleavage of the alkyl-oxygen bond to give D-Phe- ψ [(*Z*)-CF=CH]-Leu isosteres (**49** and **51**) in 40% and 66%

(40) For samarium enolate formation in the presence of aldehydes or ketones, see: (a) Molander, G. A.; Elter, J. B.; Harring, L. S.; Thorel, P.-J. *J. Am. Chem. Soc.* **1991**, *113*, 8036-8045. (b) Fukuzawa, S.; Matsuzawa, H.; Yoshimitsu, S. *J. Org. Chem.* **2000**, *65*, 1702-1706. (c) Ricci, M.; Blaksjær, P.; Skrydstrup, T. *J. Am. Chem. Soc.* **2000**, *122*, 12413-12421.

(41) Maruoka, K.; Concepcion, A. B.; Murase, N.; Oishi, M.; Hirayama, N.; Yamamoto, Y. *J. Am. Chem. Soc.* **1993**, *115*, 3943-3949.

(42) For the synthesis of β -lactones derived from amino acids and their application, see: (a) Pansare, S. V.; Huyer, G.; Arnold, L. D.; Vederas, J. C. *Org. Synth.* **1992**, *70*, 1-28. (b) Smith, N. D.; Goodman, M. *Org. Lett.* **2003**, *5*, 1035-1037.

(43) Hashimoto, N.; Aoyama, T.; Shioiri, T. *Chem. Pharm. Bull.* **1981**, *29*, 1475-1478.

SCHEME 3^a

^a Reagents and conditions: (i) 1 M LiOH (aq), THF; (ii) Ph₃P, DEAD, THF; (iii) *i*-PrMgCl, CuBr·Me₂S, Me₂S, THF, then TMSCHN₂, MeOH, benzene; (iv) BzSH, DMF, then TMSCHN₂, MeOH, benzene.

yields, respectively, without loss of chirality. Reaction of **47** and **48** with benzyl thiol in DMF, followed by esterification, also proceeded in a similar manner to afford D-Phe- ψ [(Z)-CF=CH]-Cys(Bzl) isosteres **50** and **52**, respectively.

The absolute configurations of the alkyl groups at the α -position in acyclic α -alkyl-(*E*)- β,γ -enoates can be determined by CD measurement with use of an empirical rule.⁴⁴ According to this rule, 2*S*-compounds corresponding to the D-series provide a positive Cotton effect, while 2*R*-compounds (L-series) yield a negative Cotton effect. By showing negative Cotton effects, compounds **49** and **50** were assigned (2*R*)-configurations, which correspond to (D,L)-type isosteres (D-Phe- ψ [(Z)-CF=CH]-L-Leu (or L-Cys(Bzl))). Similarly, on the basis of their positive Cotton effects, compounds **51** and **52** were assigned (2*S*)-configurations, corresponding to (D,D)-type isosteres.

(44) Ibuka, T.; Habashita, H.; Funakoshi, S.; Fujii, N.; Baba, K.; Kozawa, M.; Oguchi, Y.; Ueyehara, T.; Yamamoto, Y. *Tetrahedron: Asymmetry* 1990, 1, 389–394.

In conclusion we have devised facile methodologies for the synthesis of (*Z*)-fluoroalkene dipeptide isosteres which are potential dipeptide mimetics having structural as well as electrostatic similarity to the parent peptide bonds. The SmI₂-mediated reduction of γ,γ -difluoro- α,β -enoates was utilized to provide access to this class of mimetics. Our previous finding that γ,γ -difluoro- α,β -enoates can be reduced to γ -fluoro- δ,γ -enoates by organocopper reagents via successive single-electron-transfer processes led to our current development of the SmI₂-mediated approach toward the synthesis of (*Z*)-fluoroalkene dipeptide isosteres. By proceeding in an S_N2'-fashion, the SmI₂ reduction is likely to involve formation of dienolates, which upon kinetic trapping with proton sources (*t*-BuOH) yields Xaa-Gly-type fluoroalkene isosteres. Additionally, trapping of reduction intermediate with ketones or aldehydes affords α -substituted fluoroalkene isosteres due to the fact that highly electrophilic γ,γ -difluoro- α,β -enoates are more quickly reduced than coexisting carbonyl compounds. Furthermore, one-pot rhodium-catalyzed Reformatsky reactions of chiral aldimines and bromoacetate derivatives were successfully extended to the asymmetric synthesis of α,α -difluoro- β -amino esters, which were then subjected to the further preparation of chiral Xaa-Gly- or α -hydroxymethylated-type fluoroalkene isosteres with SmI₂-*t*-BuOH or SmI₂-HCHO protocols, respectively. Here, it is worth noting that access to various fluoroalkene isosteres possessing a wide variety of side chain functional group may be possible depending on the choice of both the aldehydes for imine formation and kinetic trapping by electrophiles or ring-opening by nucleophiles in the case of the β -lactones. Both the SmI₂-*t*-BuOH and SmI₂-carbonyl compound systems may have great synthetic applicability not only to the γ,γ -difluoro- α,β -enoates but also to other α,β -enoates possessing leaving groups at the γ -position.⁴⁵ Along this line, we are currently exploring the synthetic potential of these reaction systems. Synthetic applications of the SmI₂-mediated reactions and biological/structural evaluation of the fluoroalkene isosteres will be reported in due course.

Experimental Section

General Methods. Tetrahydrofuran (THF) was freshly distilled from sodium-benzophenone ketyl radical under a nitrogen atmosphere immediately prior to use. All reactions were conducted under a positive pressure of argon with oven-dried glassware. Melting points are uncorrected. Chemical shifts of the compounds, of which ¹H and ¹³C NMR spectra were recorded in CDCl₃, are reported in parts per million downfield from Me₄Si (s = singlet, d = doublet, dd = double doublet, ddd = doublet of double doublet, t = triplet, m = multiplet). For flash chromatographies, mixtures of silica gel 60 H (silica gel for TLC, Merck) and Wakogel C-200 (silica gel for column chromatography, Wako) were used.

Ethyl 2,2-Difluoro-3-hydroxy-4-phenylbutanoate (8a). To a stirred suspension of Zn dust (5.7 g, 86.8 mmol), activated according to published procedure,⁴⁶ in THF (50 mL) was slowly added a solution of ethyl bromodifluoroacetate (14.7 g, 72.3 mmol) in THF (30 mL) at room temperature under argon. After additional stirring for 30 min, a solution of the aldehyde **7a**

(45) Otaka, A.; Yukimasa, A.; Watanabe, J.; Sasaki, Y.; Oishi, S.; Tamamura, H.; Fujii, N. *Chem. Commun.* 2003, 1834–1835.

(46) Yeh, M. C. P.; Knochel, P. *Tetrahedron Lett.* 1988, 29, 2395–2396.

(10.0 g, 83.2 mmol) in THF (30 mL) was added to the above solution. The reaction mixture was stirred at 65 °C for 3 h, quenched at 0 °C by addition of aqueous 1 N HCl, and extracted with Et₂O. The extract was washed with 1 N HCl and brine and dried over MgSO₄. Concentration under reduced pressure followed by flash chromatography over silica gel with EtOAc-*n*-hexane (1:5) gave the title compound **8a** (6.9 g, 34% yield) as a colorless oil: ¹H NMR (270 MHz, CDCl₃) δ 1.36 (t, *J* = 7.1 Hz, 3H), 2.13 (d, *J* = 5.9 Hz, 1H), 2.83 (dd, *J* = 14.2, 10.1 Hz, 1H), 3.08 (dd, *J* = 14.2, 2.7 Hz, 1H), 4.22–4.38 (m, 1H), 4.34 (q, *J* = 7.1 Hz, 2H), 7.05–7.42 (m, 5H); ¹³C NMR (100 MHz, CDCl₃) δ 13.9, 35.5, 63.0, 72.4, 114.0, 126.7, 128.4, 129.1, 136.0, 163.0; HRMS (FAB), *m/z* calcd for C₁₇H₁₅F₂O₃ (MH⁺) 245.0989, found 245.0994.

Ethyl 3-[(*tert*-Butyl)dimethylsilyloxy]-2,2-difluoro-4-phenylbutanoate (9a). To a solution of the ester **8a** (1.8 g, 8.03 mmol) in CH₂Cl₂ (11 mL) were added 2,6-lutidine (3.7 mL, 32.1 mmol) and TBDMSOTf (3.7 mL, 16.1 mmol) at 0 °C under argon. After 2 h, the reaction mixture was extracted with EtOAc. The extract was washed with 5% NaHCO₃, 1 N HCl, and brine and dried over MgSO₄. Concentration under reduced pressure followed by flash chromatography over silica gel with EtOAc-*n*-hexane (1:20) gave the title compound **9a** (1.8 g, 68% yield) as a colorless oil: ¹H NMR (400 MHz, CDCl₃) δ -0.50 (s, 3H), -0.06 (s, 3H), 0.77 (s, 9H), 1.37 (t, *J* = 7.1 Hz, 3H), 2.80 (dd, *J* = 13.9, 9.5 Hz, 1H), 3.06 (dd, *J* = 13.9, 3.2 Hz, 1H), 4.26–4.38 (m, 3H), 7.18–7.32 (m, 5H); ¹³C NMR (100 MHz, CDCl₃) δ -5.5, -5.1, 13.9, 17.9, 25.5, 37.8, 62.6, 74.6, 114.6, 126.4, 128.0, 129.4, 136.8, 163.0; HRMS (FAB), *m/z* calcd for C₁₈H₂₁F₂O₃Si (MH⁺) 359.1854, found 359.1864.

Ethyl (2*E*)-5-[(*tert*-Butyl)dimethylsilyloxy]-4,4-difluoro-6-phenylhex-2-enoate (10a). To a solution of the ester **9a** (1.8 g, 5.02 mmol) in CH₂Cl₂ (6 mL) was added dropwise a solution of DIBAL-H in toluene (1.0 M, 6.0 mL, 6.03 mmol) at -78 °C under argon, and the mixture was stirred for 30 min. The reaction was quenched with saturated citric acid and extracted with Et₂O. The extract was washed with saturated citric acid and brine and dried over MgSO₄. Concentration under reduced pressure gave an oily aldehyde, which was used immediately in the next step without further purification. To a stirred suspension of LiCl (255 mg, 6.02 mmol) in MeCN (8 mL) under argon were added (EtO)₂P(O)CH₂CO₂Et (1.19 mL, 6.02 mmol) and (*i*-Pr)₂NEt (0.96 mL, 5.52 mmol) at 0 °C. After 20 min, the above aldehyde in MeCN (12 mL) was added to the mixture at 0 °C, and the mixture was stirred at room temperature for 4 h. The mixture was extracted with Et₂O, and the extract was washed with 0.5 N HCl and brine and dried over MgSO₄. Concentration under reduced pressure followed by flash chromatography over silica gel with EtOAc-*n*-hexane (1:20) gave the title compound **10a** (1.1 g, 56% yield) as a colorless oil: ¹H NMR (400 MHz, CDCl₃) δ -0.54 (s, 3H), -0.07 (s, 3H), 0.77 (s, 9H), 1.33 (t, *J* = 7.2 Hz, 3H), 2.55 (dd, *J* = 13.6, 9.9 Hz, 1H), 2.96 (d, *J* = 13.6 Hz, 1H), 4.05–4.13 (m, 1H), 4.26 (q, *J* = 7.2 Hz, 2H), 6.33 (d, *J* = 15.9 Hz, 1H), 6.91 (td, *J* = 15.2, 9.9 Hz, 1H), 7.15–7.30 (m, 5H); ¹³C NMR (100 MHz, CDCl₃) δ -5.6, -4.9, 14.1, 17.9, 25.6, 38.3, 61.0, 75.8, 121.9, 126.0, 126.4, 128.1, 129.6, 136.4, 136.9, 164.6; HRMS (FAB), *m/z* calcd for C₂₀H₃₁F₂O₃Si (MH⁺) 385.2010, found 385.2006.

***N*-(4-Methoxyphenyl)-2,2-difluoro-3-hydroxy-4-phenylbutanamide (11a).** To a solution of the ester **8a** (4.5 g, 18.4 mmol) in THF (20 mL) was added 1 N NaOH (20.3 mL, 20.3 mmol) at room temperature. The reaction mixture was stirred for 3 h, acidified with 3 N HCl, and extracted with EtOAc. The extract was washed with brine and dried over MgSO₄. Concentration under reduced pressure gave a pale yellow oil, which was dissolved in CH₂Cl₂ (30 mL). To the solution were added successively (*i*-Pr)₂NEt (8.0 mL, 46.0 mmol), *p*-anisidine (3.4 g, 27.6 mmol), and BOP-Cl (7.0 g, 27.6 mmol) at room temperature with additional stirring overnight. The mixture was extracted with EtOAc, and the extract was washed with 5% NaHCO₃, 1 N HCl, and brine and dried over MgSO₄.

Concentration under reduced pressure followed by flash chromatography over silica gel with EtOAc-*n*-hexane (1:5) gave the title compound **11a** (2.8 g, 46% yield) as a colorless powder: mp 135–137 °C; ¹H NMR (400 MHz, CDCl₃) δ 2.53 (d, *J* = 5.2 Hz, 1H), 2.87 (dd, *J* = 14.2, 10.3 Hz, 1H), 3.11 (d, *J* = 13.7 Hz, 1H), 3.80 (s, 3H), 4.38–4.50 (m, 1H), 6.89 (d, *J* = 8.8 Hz, 2H), 7.23–7.36 (m, 5H), 7.47 (d, *J* = 8.8 Hz, 2H), 8.01 (br, 1H); ¹³C NMR (100 MHz, CDCl₃) δ 35.6, 55.5, 72.1, 114.2, 115.3, 122.0, 126.8, 128.5, 128.7, 129.3, 136.3, 157.2, 161.0. Anal. Calcd for C₁₇H₁₇F₂NO₃: C, 63.54; H, 5.33; N, 4.36. Found: C, 63.51; H, 5.37; N, 4.30.

***N*-(4-Methoxyphenyl)-3-benzyl-2,2-difluoropropano-3-lactam (12a).** To a solution of Ph₃P (3.4 g, 12.9 mmol) and the amide **11a** (2.7 g, 8.60 mmol) in THF (20 mL) was added a solution of DEAD in toluene (40%, 5.1 mL, 11.2 mmol) at 0 °C under argon. After 1.5 h, the reaction mixture was concentrated under reduced pressure and purified by flash chromatography over silica gel with EtOAc-*n*-hexane (1:8) to give the title compound **12a** (2.2 g, 85% yield) as colorless crystals: mp 118–120 °C; ¹H NMR (400 MHz, CDCl₃) δ 3.10 (dd, *J* = 14.9, 9.3 Hz, 1H), 3.26 (d, *J* = 12.9 Hz, 1H), 3.81 (s, 3H), 4.59–4.66 (m, 1H), 6.89 (d, *J* = 9.0 Hz, 2H), 7.23–7.36 (m, 7H); ¹³C NMR (100 MHz, CDCl₃) δ 33.0, 55.5, 66.5, 114.6, 119.7, 120.0, 127.2, 128.2, 128.7, 128.8, 135.1, 156.7, 157.3. Anal. Calcd for C₁₇H₁₅F₂NO₂: C, 67.32; H, 4.98; N, 4.62. Found: C, 67.37; H, 5.05; N, 4.45.

Methyl 2,2-Difluoro-3-[*N*-(4-methoxyphenyl)amino]-4-phenylbutanoate (13a). To a solution of the lactam **12a** (2.2 g, 7.29 mmol) in THF (10 mL) was added 1 N NaOH (7.6 mL, 7.60 mmol) at room temperature. After 2 h, the mixture was concentrated under reduced pressure to give an oily residue, which was dissolved in MeOH (80 mL). To the solution was added concentrated H₂SO₄ at room temperature. The reaction mixture was stirred for 3 h under reflux and extracted with Et₂O. The extract was washed with saturated NaHCO₃ and brine and dried over MgSO₄. Concentration under reduced pressure followed by flash chromatography over silica gel with EtOAc-*n*-hexane (1:8) gave the title compound **13a** (2.4 g, 99% yield) as a pale yellow oil: ¹H NMR (400 MHz, CDCl₃) δ 2.84 (dd, *J* = 14.2, 8.6 Hz, 1H), 3.16 (dd, *J* = 14.3, 4.8 Hz, 1H), 3.67 (s, 3H), 3.70 (s, 3H), 4.16–4.28 (m, 1H), 6.45 (d, *J* = 9.0 Hz, 2H), 6.66 (d, *J* = 8.8 Hz, 2H), 7.16–7.25 (m, 5H); ¹³C NMR (100 MHz, CDCl₃) δ 34.8, 53.1, 55.5, 60.2, 114.3, 115.4, 126.4, 128.1, 129.1, 136.3, 139.7, 152.6, 164.0; HRMS (FAB), *m/z* calcd for C₁₈H₁₉F₂NO₃ (M⁺) 335.1333, found 335.1340.

Methyl 3-[*N*-(*tert*-Butoxycarbonyl)amino]-2,2-difluoro-4-phenylbutanoate (14a). To a solution of the ester **13a** (400 mg, 1.19 mmol) in MeCN (7 mL) was added a solution of CAN (1.96 g, 3.58 mmol) in H₂O (5 mL) at 0 °C. The reaction mixture was stirred for 20 min at 0 °C and then at room temperature for 3 h. To the reaction mixture was added 3-mercaptopropionic acid (0.520 mL, 5.97 mmol) at room temperature. After 30 min, the reaction mixture was extracted with EtOAc. The extract was washed with saturated NaHCO₃ and brine and dried over MgSO₄. Concentration under reduced pressure gave an oily residue, which was dissolved in THF (10 mL). To the solution was added (Boc)₂O (500 mg, 2.38 mmol) and the mixture was stirred for 4 h under reflux. Concentration under reduced pressure followed by flash chromatography over silica gel with EtOAc-*n*-hexane (1:10) gave the title compound **14a** (175 mg, 44% yield) as colorless crystals: mp 84–86 °C; ¹H NMR (400 MHz, CDCl₃) δ 1.30 (s, 9H), 2.71 (dd, *J* = 14.0, 9.8 Hz, 1H), 3.14 (dd, *J* = 14.9, 2.9 Hz, 1H), 3.82 (s, 3H), 4.59 (br, 2H), 7.19–7.33 (m, 5H); ¹³C NMR (100 MHz, CDCl₃) δ 28.0, 33.9, 53.3, 53.6, 80.1, 114.1, 126.6, 128.2, 128.9, 135.4, 154.4, 163.2. Anal. Calcd for C₁₆H₂₁F₂NO₄: C, 58.35; H, 6.43; N, 4.25. Found: C, 58.10; H, 6.36; N, 4.28.

Ethyl (2*E*)-5-[*N*-(*tert*-Butoxycarbonyl)amino]-4,4-difluoro-6-phenylhex-2-enoate (15a). To a solution of the ester **14a** (685 mg, 2.08 mmol) in CH₂Cl₂ (5 mL) was added dropwise a solution of DIBAL-H in toluene (1.0 M, 4.1 mL, 4.16 mmol) at -78 °C under argon, and the mixture was

stirred for 30 min at -78°C . The reaction was quenched with saturated citric acid and extracted with Et₂O. The extract was washed with saturated citric acid and brine and dried over MgSO₄. Concentration under reduced pressure gave an oily aldehyde, which was used immediately in the next step without further purification. To a stirred suspension of LiCl (123 mg, 2.91 mmol) in MeCN (6 mL) under argon were added (EtO)₂P(O)CH₂CO₂Et (0.577 mL, 2.91 mmol) and (*i*-Pr)₂NEt (0.506 mL, 2.91 mmol) at 0°C . After 20 min, the above aldehyde in MeCN (6 mL) was added to the mixture at 0°C , and the mixture was stirred at room temperature for 4 h. The mixture was extracted with Et₂O, and the extract was washed with 0.5 N HCl and brine and dried over MgSO₄. Concentration under reduced pressure followed by flash chromatography over silica gel with EtOAc-*n*-hexane (1:6) gave the title compound **15a** (515 mg, 67% yield) as colorless crystals: mp $93\text{--}95^\circ\text{C}$; ¹H NMR (400 MHz, CDCl₃) δ 1.28 (s, 9H), 1.30 (t, $J = 7.1$ Hz, 3H), 2.67 (t, $J = 12.6$ Hz, 1H), 3.18 (dd, $J = 14.5, 3.8$ Hz, 1H), 4.23 (q, $J = 7.2$ Hz, 2H), 4.34 (br, 1H), 4.51 (d, $J = 9.3$ Hz, 1H), 6.33 (d, $J = 15.9$ Hz, 1H), 6.85 (dt, $J = 15.6, 11.9$ Hz, 1H), 7.18–7.32 (m, 5H); ¹³C NMR (100 MHz, CDCl₃) δ 14.1, 28.0, 34.2, 55.1, 61.0, 80.0, 119.3, 126.1, 126.5, 128.2, 128.8, 135.9, 137.0, 154.6, 164.3. Anal. Calcd for C₁₉H₂₅F₂NO₄: C, 61.78; H, 6.82; N, 3.79. Found: C, 61.85; H, 6.93; N, 3.78.

General Procedure for the Preparation of Organo-copper Reagent (Me₂CuLi·LiCN·2LiCl·2LiBr) and Reduction of γ,γ -Difluoro- α,β -enoate: Synthesis of Ethyl (3Z)-5-[(*tert*-Butyl)dimethylsiloxy]-4-fluoro-6-phenylhex-3-enoate (16a**) (Table 1, entry 1).** To a solution LiCl (44 mg, 1.04 mmol) and CuCN (46 mg, 0.520 mmol) in THF (0.5 mL) was added a solution of MeLi·LiBr in Et₂O (1.5 M, 0.693 mL, 1.04 mmol) at -78°C under argon with additional stirring for 10 min. The mixture was allowed to warm to 0°C and then stirred for 10 min at this temperature. To the recooled solution of the organocopper reagent to -78°C was added a solution of the enoate **10a** (50 mg, 0.130 mmol) in THF (1 mL) under argon. The reaction was continued for 10 min and then quenched at 0°C by addition of saturated NH₄Cl–28% NH₄OH solution (1:1) with additional stirring at room temperature for 30 min. The mixture was extracted with Et₂O, and the extract was washed with brine and dried over MgSO₄. Concentration under reduced pressure followed by flash chromatography over silica gel with EtOAc-*n*-hexane (1:20) gave a mixture of **16a** and **17a** (31 mg, 69% combined yield, **16a**:**17a** = 59:10).

Compound 16a: colorless oil; ¹H NMR (400 MHz, CDCl₃) δ -0.29 (s, 3H), -0.09 (s, 3H), 0.82 (s, 9H), 1.25 (t, $J = 7.0$ Hz, 3H), 2.79 (dd, $J = 13.3, 8.4$ Hz, 1H), 2.98 (dd, $J = 13.4, 4.2$ Hz, 1H), 3.12 (t, $J = 7.8$ Hz, 2H), 4.13 (q, $J = 7.1$ Hz, 2H), 4.22 (m, 1H), 5.01 (dt, $J = 36.4, 7.3$ Hz, 1H), 7.16–7.29 (m, 5H); ¹³C NMR (100 MHz, CDCl₃) δ $-5.4, -5.0, 14.3, 18.2, 25.9, 29.4, 42.1, 60.8, 72.3, 98.2, 128.2, 129.7, 137.7, 159.8, 170.8$; HRMS (FAB), m/z calcd for C₂₀H₃₂F₂O₃Si (MH⁺) 367.2105, found 367.2084.

Compound 17a: colorless oil; ¹H NMR (270 MHz, CDCl₃) δ 1.26 (t, $J = 7.2$ Hz, 3H), 3.52 (d, $J = 8.6$ Hz, 2H), 4.52 (q, $J = 7.0$ Hz, 2H), 5.67 (dt, $J = 19.2, 8.5$ Hz, 1H), 6.20 (d, $J = 15.7$ Hz, 1H), 7.16–7.32 (m, 5H), 7.44 (d, $J = 15.7$ Hz, 1H).

Essentially same procedure was used in experiments in Table 1, entry 2 and in Table 2, entries 1 and 2.

General Procedure for the Preparation of 0.1 M SmI₂ in THF and Reduction of γ,γ -Difluoro- α,β -enoate (Table 1, entry 4). To a suspension of Sm powder (240 mg, 1.60 mmol) in THF (4 mL) was added a solution of CH₂I₂ (0.064 mL, 0.800 mmol) in THF (4 mL) at room temperature under argon. The mixture was stirred for 1 h. To a solution of the enoate **10a** (40 mg, 0.104 mmol) in THF–EtOH (3:1, 2 mL) was added the above solution of SmI₂ in THF (0.1 M, 6.2 mL, 0.624 mmol) at 0°C under argon. After 1 h, the reaction mixture was quenched with saturated NH₄Cl and extracted with Et₂O. The extract was washed with saturated NH₄Cl and brine and dried

over MgSO₄. Concentration under reduced pressure followed by flash chromatography over silica gel with EtOAc-*n*-hexane (1:20) gave 35 mg (92% yield) of the mixture of the enoate **16a** and the ester **18a**. The product ratio was determined by ¹H NMR analysis (**16a**:**18a** = 73:27).

Compound 18a: colorless oil; ¹H NMR (400 MHz, CDCl₃) δ -0.55 (s, 3H), -0.09 (s, 3H), 0.77 (s, 9H), 1.28 (t, $J = 7.1$ Hz, 3H), 2.12–2.48 (m, 2H), 2.55–2.65 (m, 3H), 2.91–3.02 (m, 1H), 3.96–4.05 (m, 1H), 4.16 (q, $J = 7.2$ Hz, 2H), 7.16–7.29 (m, 5H); HRMS (FAB), m/z calcd for C₂₀H₃₃F₂O₃Si (MH⁺) 387.2167, found 387.2171.

A procedure similar to that described above was used in experiments in Table 1, entry 5. Similar SmI₂-mediated reductions with *t*-BuOH as the proton source were applied to experiments in Table 1, entries 6–9. For the SmI₂-*t*-BuOH reduction protocol, see the following section.

Ethyl (3Z)-5-[*N*-(*tert*-Butoxycarbonyl)amino]-4-fluoro-6-phenylhex-3-enoate (23a**) (Table 2, entry 3).** To a solution of the enoate **15a** (40 mg, 0.108 mmol) in THF-*t*-BuOH (3:1, 2 mL) was added a solution of SmI₂ in THF (0.1 M, 6.5 mL, 0.649 mmol) at 0°C under argon. After 1 h, the reaction mixture was quenched with saturated NH₄Cl and extracted with Et₂O. The extract was washed with saturated NH₄Cl and brine and dried over MgSO₄. Concentration under reduced pressure followed by flash chromatography over silica gel with EtOAc-*n*-hexane (1:7) gave the title compound **23a** (36 mg, 92% yield) as colorless crystals: mp $60\text{--}61^\circ\text{C}$; ¹H NMR (400 MHz, CDCl₃) δ 1.24 (t, $J = 7.1$ Hz, 3H), 1.39 (s, 9H), 2.86–2.96 (m, 2H), 3.01–3.15 (m, 2H), 4.11 (q, $J = 7.1$ Hz, 2H), 4.49 (br, 1H), 4.68 (br, 1H), 4.87 (dt, $J = 36.4, 7.2$ Hz, 1H), 7.16–7.31 (m, 5H); ¹³C NMR (100 MHz, CDCl₃) δ 14.1, 28.2, 29.3, 38.5, 52.4, 60.7, 79.7, 99.1, 126.4, 128.1, 129.0, 136.1, 154.3, 158.2, 170.4. Anal. Calcd for C₁₉H₂₆FNO₄: C, 64.94; H, 7.46; N, 3.99. Found: C, 64.69; H, 7.40; N, 3.77.

Ethyl (3S)-2,2-Difluoro-3-[(*N*-(1*R*)-(2-methoxy-1-phenylethyl)amino)-4-methylpentanoate (27**).** A solution of the aldehyde **24** (144 mg, 2.00 mmol) and the amine **25** (320 mg, 2.06 mmol) in THF (5 mL) was stirred at 0°C for 4 h under argon in the presence of activated molecular sieves 3Å. To the mixture were successively added a suspension of Wilkinson's catalyst (92 mg, 0.100 mmol) in THF (6 mL), BrCF₂CO₂Et (0.281 mL, 2.20 mmol), and a solution of Et₂Zn in hexane (1.0 M, 8.0 mL, 8.00 mmol). After being stirred for 30 min at 0°C , the reaction was quenched with saturated NaHCO₃. The mixture was filtered over Celite and the filtrate was extracted with EtOAc. The extract was washed with saturated NaHCO₃ and brine and dried over MgSO₄. Concentration under reduced pressure followed by flash chromatography over silica gel with EtOAc-*n*-hexane (1:10) gave the title compound **27** (333 mg, 50% yield) as a colorless oil: $[\alpha]_D^{25} -56.1$ (c 0.93, CHCl₃); ¹H NMR (270 MHz, CDCl₃) δ 0.84 (d, $J = 6.6$ Hz, 3H), 0.88 (d, $J = 6.9$ Hz, 3H), 1.32 (t, $J = 7.1$ Hz, 3H), 1.63–1.80 (m, 1H), 2.92 (ddd, $J = 15.6, 12.6, 2.9$ Hz, 1H), 3.35 (dd, $J = 9.9, 4.3$ Hz, 1H), 3.38 (s, 3H), 3.47 (t, $J = 9.1$ Hz, 1H), 4.28–4.36 (m, 1H), 4.30 (q, $J = 7.1$ Hz, 2H), 7.23–7.38 (m, 5H); ¹³C NMR (100 MHz, CDCl₃) δ 13.9, 16.2, 21.1, 58.6, 59.9, 60.3, 62.7, 77.9, 118.0, 127.6, 128.1, 128.2, 139.9, 164.2; HRMS (FAB), m/z calcd for C₁₇H₂₆F₂NO₃ (MH⁺) 330.1881, found 330.1874.

Ethyl (3S)-3-[*N*-(*tert*-Butoxycarbonyl)amino]-2,2-difluoro-4-methylpentanoate (28**).** To a solution of the ester **27** (820 mg, 2.49 mmol) in EtOH (10 mL) was added 20% palladium hydroxide on carbon (500 mg), and the suspension was stirred for 4 h under H₂ at room temperature. The mixture was filtered through a pad of Celite and the filtrate was concentrated under reduced pressure to give a colorless oil, which was dissolved in THF (10 mL). To the solution was added (Boc)₂O (1.09 g, 4.98 mmol) and the mixture was stirred for 6 h under reflux. Concentration under reduced pressure followed by flash chromatography over silica gel with EtOAc-*n*-hexane (1:10) gave the title compound **28** (500 mg, 68% yield) as a colorless oil: $[\alpha]_D^{25} -10.9$ (c 1.01, CHCl₃); ¹H NMR (270

MHz, CDCl₃) δ 0.95 (d, *J* = 6.9 Hz, 3H), 1.01 (d, *J* = 6.5 Hz, 3H), 1.34 (t, *J* = 7.0 Hz, 3H), 1.43 (s, 9H), 2.02–2.19 (m, 1H), 4.10–4.25 (m, 1H), 4.31 (q, *J* = 6.7 Hz, 2H), 4.69 (d, *J* = 10.6 Hz, 1H); ¹³C NMR (100 MHz, CDCl₃) δ 14.3, 17.3, 22.8, 28.3, 56.5, 63.1, 80.1, 115.1, 155.2, 163.3; HRMS (FAB), *m/z* calcd for C₁₃H₂₃F₂NO₄ (MH⁺) 296.1673, found 296.1678.

Ethyl (5*S*,2*E*)-5-[*N*-(*tert*-Butoxycarbonyl)amino]-4,4-difluoro-6-methylhept-2-enoate (29). By use of a procedure similar to that described for the preparation of the enoate 15a, the ester 28 (290 mg, 0.982 mmol) was converted into the title compound 29 (260 mg, 82% yield) as colorless crystals: mp 43–44 °C; [α]_D²⁰ –5.0 (*c* 1.00, CHCl₃); ¹H NMR (270 MHz, CDCl₃) δ 0.94 (d, *J* = 6.6 Hz, 3H), 1.00 (d, *J* = 6.9 Hz, 3H), 1.30 (t, *J* = 7.1 Hz, 3H), 1.44 (s, 9H), 2.08–2.22 (m, 1H), 3.85–4.04 (m, 1H), 4.23 (q, *J* = 7.0 Hz, 2H), 4.67 (d, *J* = 10.6 Hz, 1H), 6.30 (d, *J* = 15.8 Hz, 1H), 6.82 (dt, *J* = 15.8, 11.8 Hz, 1H); ¹³C NMR (100 MHz, CDCl₃) δ 14.3, 17.0, 22.8, 28.3, 58.2, 61.1, 80.1, 120.0, 122.5, 137.9, 155.5, 164.6. Anal. Calcd for C₁₅H₂₅F₂NO₄: C, 56.06; H, 7.84; N, 4.36. Found: C, 55.86; H, 7.74; N, 4.35.

Ethyl (5*S*,3*Z*)-5-[*N*-(*tert*-Butoxycarbonyl)amino]-4-fluoro-6-methylhept-3-enoate (30). By use of a procedure similar to that described for SmI₂-mediated reduction of γ,γ -difluoro- α,β -enoate 15a (Table 2, entry 3), the enoate 29 (50 mg, 0.156 mmol) was converted into the title compound 30 (40 mg, 85% yield) as a colorless oil: [α]_D²⁰ –30.5 (*c* 1.02, CHCl₃); ¹H NMR (270 MHz, CDCl₃) δ 0.94 (d, *J* = 2.0 Hz, 3H), 0.96 (d, *J* = 2.0 Hz, 3H), 1.26 (t, *J* = 7.1 Hz, 3H), 1.45 (s, 9H), 1.83–1.98 (m, 1H), 3.09–3.17 (m, 2H), 3.90–4.07 (m, 1H), 4.14 (q, *J* = 7.0 Hz, 2H), 4.72 (d, *J* = 9.2 Hz, 1H), 4.98 (dt, *J* = 36.6, 7.1 Hz, 1H); ¹³C NMR (100 MHz, CDCl₃) δ 14.2, 18.3, 19.4, 21.1, 28.3, 29.4, 57.3, 60.4, 79.7, 99.2, 155.0, 158.8, 170.8; HRMS (FAB), *m/z* calcd for C₁₅H₂₇FNO₄ (MH⁺) 304.1924, found 304.1935.

Ethyl (5*R*,3*Z*)-5-[*N*-(*tert*-Butoxycarbonyl)amino]-4-fluoro-6-phenylhex-3-enoate (35): colorless crystals; mp 60–61 °C; [α]_D²⁰ –8.8 (*c* 0.80, CHCl₃); ¹H NMR and ¹³C NMR same as compound 23a. Anal. Calcd for C₁₉H₂₆FNO₄: C, 64.94; H, 7.46; N, 3.99. Found: C, 64.69; H, 7.40; N, 3.77.

***N*-(1*R*)-1-Phenylethyl]-5*S*,2*E*)-5-[*N*-(*tert*-butoxycarbonyl)amino]-4,4-difluoro-6-methylhept-2-enamide (31).** To a solution of the enoate 29 (100 mg, 0.311 mmol) in THF (0.4 mL) was added 1 N LiOH (0.342 mL, 0.342 mmol) at room temperature. The mixture was stirred for 1 h and extracted with EtOAc after acidification with 1 N HCl. The extract was washed with brine and dried over MgSO₄. Concentration under reduced pressure gave an oily residue, which was dissolved in THF (2 mL). To the solution were added (*R*)-methylbenzylamine (0.044 mL, 0.342 mmol), (*i*-Pr)₂NEt (0.059 mL, 0.342 mmol), 1-hydroxybenzotriazole (52 mg, 0.342 mmol), and 1-ethyl-3-(3'-dimethylaminopropyl)carbodiimide (0.059 mL, 0.342 mmol) at room temperature. The mixture was stirred overnight and extracted with EtOAc. The extract was washed with saturated citric acid, saturated NaHCO₃, and brine and dried over MgSO₄. Concentration under reduced pressure gave solid materials. Recrystallization of the solid from EtOAc-*n*-hexane gave the title compound 31 (60 mg, 48% yield) as colorless crystals: mp 188–190 °C; [α]_D¹⁴ +13.3 (*c* 0.08, CHCl₃); ¹H NMR (400 MHz, CDCl₃) δ 0.91 (d, *J* = 6.8 Hz, 3H), 0.98 (d, *J* = 6.8 Hz, 3H), 1.41 (s, 9H), 1.54 (s, 3H), 2.08–2.19 (m, 1H), 3.88–4.00 (m, 1H), 4.67 (d, *J* = 11.0 Hz, 1H), 5.16–5.24 (m, 1H), 5.91 (d, *J* = 7.3 Hz, 1H), 6.28 (d, *J* = 15.6 Hz, 1H), 6.74 (dt, *J* = 15.1, 11.5 Hz, 1H), 7.25–7.38 (m, 5H); HRMS (FAB), *m/z* calcd for C₂₁H₃₁F₂N₃O₃ (MH⁺) 397.2303, found 397.2292.

Ethyl (5*R*,3*Z*)-5-[*N*-(*tert*-Butoxycarbonyl)amino]-4-fluoro-2-(1-hydroxy-1-methylethyl)-6-phenylhex-3-enoate (43) (Table 3, entry 2). To a mixture containing the enoate 34 (40 mg, 0.106 mmol) and acetone (0.024 mL, 0.324 mmol) in THF (1.5 mL) was added a solution of SmI₂ in THF (0.1 M, 3.2 mL, 0.324 mmol) at 0 °C under argon. After 1 h, the reaction mixture was quenched with saturated NH₄Cl and extracted with Et₂O. The extract was washed with saturated

NH₄Cl and brine and dried over MgSO₄. Concentration under reduced pressure followed by flash chromatography over silica gel with EtOAc-*n*-hexane (1:3) gave 37 mg (82%) of a mixture of diastereomers of the title compound 43 as a colorless oil: ¹H NMR (400 MHz, CDCl₃) δ 0.96 (s, 1.5H), 1.10 (s, 3H), 1.21 (s, 1.5H), 1.25 (t, *J* = 7.2 Hz, 1.5H), 1.27 (t, *J* = 7.1 Hz, 1.5H), 1.40 (s, 4.5H), 1.41 (s, 4.5H), 2.86–3.02 (m, 1H), 3.42 (d, *J* = 7.1 Hz, 0.5H), 3.44 (d, *J* = 7.1 Hz, 0.5H), 4.07–4.22 (m, 2H), 4.50 (br, 1H), 4.69 (br, 1H), 4.86 (dd, *J* = 35.6, 10.4 Hz, 0.5H), 4.89 (dd, *J* = 35.6, 10.4 Hz, 0.5H), 7.14–7.30 (m, 5H); ¹³C NMR (100 MHz, CDCl₃) δ 14.1, 26.2, 26.4, 28.2, 38.3, 50.5, 52.9, 60.9, 71.4, 79.9, 102.0, 128.1, 128.2, 129.0, 136.0, 154.2, 161.6, 171.6; HRMS (FAB), *m/z* calcd for C₂₂H₃₃FNO₃ (MH⁺) 410.2343, found 410.2353.

Ethyl (5*R*,3*Z*)-5-[*N*-(*tert*-Butoxycarbonyl)amino]-2-ethoxycarbonyl-4-fluoro-6-phenylhex-3-enoate (44) (Table 3, entry 3). To a mixture containing the enoate 34 (80 mg, 0.217 mmol) and (EtOCO)₂O (0.157 mL, 1.09 mmol) in THF (2.0 mL) was added a solution of SmI₂ in THF (0.1 M, 13.0 mL, 1.30 mmol) at 0 °C under argon. After 1 h, the reaction mixture was quenched with saturated NH₄Cl and extracted with Et₂O. The extract was washed with saturated NH₄Cl and brine and dried over MgSO₄. Concentration under reduced pressure followed by flash chromatography over silica gel with EtOAc-*n*-hexane (1:6) gave the title compound 44 (70 mg, 76% yield) as a colorless oil: [α]_D²⁰ –8.2 (*c* 0.86, CHCl₃); ¹H NMR (270 MHz, CDCl₃) δ 1.24 (t, *J* = 7.1 Hz, 3H), 1.26 (t, *J* = 6.6 Hz, 3H), 1.39 (s, 9H), 2.95 (d, *J* = 5.9 Hz, 2H), 4.11–4.23 (m, 4H), 4.40 (d, *J* = 9.6 Hz, 1H), 4.55 (br, 1H), 4.68 (d, *J* = 8.9 Hz, 1H), 5.07 (dd, *J* = 35.3, 9.6 Hz, 1H), 7.14–7.33 (m, 5H); ¹³C NMR (100 MHz, CDCl₃) δ 14.1, 28.4, 38.5, 47.8, 52.3, 61.8, 61.9, 80.0, 99.4, 126.7, 128.3, 129.2, 135.9, 154.4, 159.7, 166.9, 167.1; HRMS (FAB), *m/z* calcd for C₂₂H₃₁FNO₆ (MH⁺) 424.2135, found 424.2141.

Ethyl (5*R*,3*Z*)-5-[*N*-(*tert*-Butoxycarbonyl)amino]-4-fluoro-2-hydroxymethyl-6-phenylhex-3-enoate (45) (Table 3, entry 4). To a solution of 2,6-diphenylphenol (800 mg, 3.25 mmol) in CH₂Cl₂ (8 mL) was added a solution of Me₃Al in *n*-hexane (1.02 M, 1.59 mL, 1.62 mmol) at room temperature under argon. After 1 h, a solution of *s*-trioxane (48 mg, 0.541 mmol) in CH₂Cl₂ (2 mL) was added to the reaction mixture at 0 °C. After 1 h, to the reaction mixture were successively added a solution of the enoate 34 (100 mg, 0.271 mmol) in THF (2 mL) and a solution of SmI₂ in THF (0.1 M, 8.1 mL, 0.812 mmol) at 0 °C. After being stirred for 1 h at the same temperature, the reaction mixture was quenched with saturated NH₄Cl and extracted in the usual manner. Purification by flash chromatography over silica gel with EtOAc-*n*-hexane (1:2) gave the title compound (mixture of diastereomer) 45 (67 mg, 65% yield) as a colorless oil: ¹H NMR (600 MHz, CDCl₃) δ 1.24 (t, *J* = 7.1 Hz, 1.5H), 1.25 (t, *J* = 7.1 Hz, 1.5H), 1.40 (s, 4.5H), 1.42 (s, 4.5H), 2.86–3.00 (m, 2H), 3.52–3.63 (m, 2H), 3.65–3.68 (m, 0.5H), 3.71–3.76 (m, 0.5H), 4.08–4.20 (m, 2H), 4.46 (br, 1H), 4.63–4.76 (br, 1H), 4.70 (dd, *J* = 37.0, 9.3 Hz, 0.5H), 4.76 (dd, *J* = 36.4, 9.6 Hz, 0.5H), 7.17 (d, *J* = 7.2 Hz, 2H), 7.21–7.32 (m, 3H); ¹³C NMR (100 MHz, CDCl₃) δ 14.1, 28.2, 38.4, 43.4, 53.0, 61.0, 63.0, 79.9, 101.6, 126.6, 128.1, 128.2, 135.8, 153.8, 157.3, 171.9; HRMS (FAB), *m/z* calcd for C₂₀H₂₉FNO₅ (MH⁺) 382.2030, found 382.2023.

(2*S*)-2-[(3*R*,1*Z*)-3-[*N*-(*tert*-Butoxycarbonyl)amino]-2-fluoro-4-phenylbut-1-enyl]propano-3-lactone (47) and Its (2*R*)-Diastereomer (48). To a solution of the enoate 45 (63 mg, 0.189 mmol) in THF (0.2 mL) was added 1 N LiOH (0.182 mL, 0.182 mmol) at room temperature. After 3 h, the reaction mixture was acidified with 1 N HCl and extracted with EtOAc. The extract was washed with brine and dried over MgSO₄. Concentration under reduced pressure gave the oily carboxylic acid 46. To a solution of Ph₃P (43 mg, 0.167 mmol) and 46 in THF (0.5 mL) was added a solution of DEAD in toluene (40%, 0.075 mL, 0.167 mmol) at –78 °C under argon. After 10 min of stirring at –78 °C, a solution of the above carboxylic acid in THF (1 mL) was added to the mixture at

–78 °C. After 2 h, the reaction mixture was concentrated under reduced pressure and purified by flash chromatography over silica gel with EtOAc–*n*-hexane (1:3) to give the title compound **47** and its diastereomer **48** (total 19 mg, 37% yield, **47**:**48** = 1:1).

Compound 47: colorless crystals; mp 82–84 °C; $[\alpha]_D^{25}$ –9.3 (c 0.32, CHCl₃); ¹H NMR (400 MHz, CDCl₃) δ 1.40 (s, 9H), 2.95 (d, *J* = 6.8 Hz, 2H), 4.05 (t, *J* = 5.0 Hz, 1H), 4.43 (t, *J* = 6.0 Hz, 1H), 4.44 (br, 1H), 4.54 (br, 1H), 4.68 (br, 1H), 4.84 (dd, *J* = 35.2, 8.6 Hz, 1H), 7.13–7.34 (m, 5H); ¹³C NMR (100 MHz, CDCl₃) δ 28.4, 38.5, 47.6, 52.7, 65.0, 80.3, 98.6, 126.9, 128.4, 129.2, 135.7, 154.4, 160.6, 168.4. Anal. Calcd for C₁₈H₂₂FNO₄: C, 64.46; H, 6.61; N, 4.18. Found: C, 64.18; H, 6.72; N, 4.04.

Compound 48: colorless crystals; mp 107–110 °C; $[\alpha]_D^{25}$ +97.7 (c 0.13, CHCl₃); ¹H NMR (400 MHz, CDCl₃) δ 1.40 (s, 9H), 2.95 (d, *J* = 6.6 Hz, 2H), 3.95 (t, *J* = 4.9 Hz, 1H), 4.41 (dd, *J* = 6.8, 5.1 Hz, 1H), 4.50 (br, 1H), 4.56–4.62 (m, 1H), 4.64 (br, 1H), 4.82 (dd, *J* = 34.9, 8.8 Hz, 1H), 7.14–7.32 (m, 5H); ¹³C NMR (100 MHz, CDCl₃) δ 28.4, 38.3, 47.4, 52.5, 65.0, 80.3, 98.5, 126.9, 128.5, 129.2, 135.7, 154.4, 160.7, 168.5. Anal. Calcd for C₁₈H₂₂FNO₄: C, 64.46; H, 6.61; N, 4.18. Found: C, 64.43; H, 6.78; N, 3.96.

Methyl (2*R*,5*R*,3*Z*)-5-[*N*-(*tert*-Butoxycarbonyl)amino]-4-fluoro-2-(2-methylpropyl)-6-phenylhex-3-enoate (49). To a mixture consisting of β -lactone **47** (18 mg, 0.0537 mmol) and CuBr·Me₂S (3.3 mg, 0.0161 mmol) in THF–Me₂S (0.840 mL, 20:1) was added dropwise a solution of *i*-PrMgCl in Et₂O (0.32 mL, 0.32 mmol) at –23 °C under argon. After being stirred for 1 h at –23 °C, the reaction mixture was quenched with 1 N HCl and extracted with EtOAc. The extract was washed with brine, dried over MgSO₄, and concentrated under reduced pressure to give an oil. To a solution of the above oil in MeOH–benzene (0.3 mL, 1:2) was added TMSCHN₂ in hexane (2.0 M, 0.080 mL, 0.161 mmol) at room temperature. After 3 h, the reaction mixture was quenched with AcOH and extracted with EtOAc. The extract was washed with 5% NaHCO₃ and brine and dried over MgSO₄. Concentration under reduced pressure followed by flash chromatography over silica gel with EtOAc–*n*-hexane (1:8) gave the title compound **49** (9 mg, 40% yield) as a colorless oil: $[\alpha]_D^{25}$ –17.5 (c 0.46, CHCl₃); $\Delta\epsilon$ = –2.34 (214 nm, isooctane); ¹H NMR (400 MHz, CDCl₃) δ 0.86 (t, *J* = 6.6 Hz, 6H), 1.26–1.54 (m, 3H), 1.40 (s, 9H), 2.92 (d, *J* = 7.1 Hz, 2H), 3.50 (br, 1H), 3.60 (s, 3H), 4.45 (br, 1H), 4.63 (dd, *J* = 36.3, 10.1 Hz, 1H), 4.65 (br, 1H), 7.13–7.30 (m, 5H); ¹³C NMR (100 MHz, CDCl₃) δ 21.9, 22.8, 25.7, 28.4, 38.5, 39.0, 41.5, 51.9, 52.8, 79.9, 105.6, 126.6, 128.2, 129.2, 136.2, 154.5, 157.8, 173.9; HRMS (FAB), *m/z* calcd for C₂₂H₃₃FNO₄ (MH⁺) 394.2393, found 394.2403.

Methyl (2*S*,5*R*,3*Z*)-5-[*N*-(*tert*-Butoxycarbonyl)amino]-4-fluoro-2-(2-methylpropyl)-6-phenylhex-3-enoate (51). By use of a procedure similar to that described for the preparation of the ester **49**, the β -lactone **48** (18 mg, 0.0537 mmol) was converted into the title compound **51** (14 mg, 66% yield) as a colorless oil: $[\alpha]_D^{25}$ +33.4 (c 0.69, CHCl₃); $\Delta\epsilon$ = +3.01 (217 nm, isooctane); ¹H NMR (400 MHz, CDCl₃) δ 0.80 (t, *J* = 5.6 Hz, 6H), 1.15–1.30 (m, 3H), 1.41 (s, 9H), 2.88 (dd, *J* = 13.7, 8.1 Hz, 1H), 2.95 (br, 1H), 3.43–3.51 (m, 1H), 3.64 (s, 3H), 4.46 (br, 1H), 4.60 (dd, *J* = 36.2, 10.1 Hz, 1H), 4.70 (br, 1H), 7.13–7.30 (m, 5H); ¹³C NMR (100 MHz, CDCl₃) δ 21.7, 22.8, 25.3, 28.4, 38.4, 38.7, 41.3, 51.7, 52.8, 79.8, 105.5, 126.4, 128.1, 129.1, 136.1, 154.3, 157.3, 173.8; HRMS (FAB), *m/z* calcd for C₂₂H₃₃FNO₄ (MH⁺) 394.2393, found 394.2387.

Methyl (2*R*,5*R*,3*Z*)-2-Benzylsulfanylmethyl-5-[*N*-(*tert*-butoxycarbonyl)amino]-4-fluoro-6-phenylhex-3-enoate (50). To a solution of β -lactone **47** (5 mg, 0.0149 mmol) in DMF (0.2 mL) was added benzylmercaptan (0.010 mL, 0.0596 mmol) at room temperature. After 60 h at room temperature, the reaction mixture was extracted with EtOAc and the extract was washed with 1 N HCl and brine, dried over MgSO₄, and concentrated under reduced pressure to give an oil. To a solution of the above oil in MeOH–benzene (0.1 mL, 1:2) was added TMSCHN₂ in hexane (2.0 M, 0.022 mL, 0.0447 mmol) at room temperature. After 3 h, the reaction mixture was quenched with AcOH and extracted with EtOAc. The extract was washed with brine and dried over MgSO₄. Concentration under reduced pressure followed by flash chromatography over silica gel with EtOAc–*n*-hexane (1:6) gave the title compound **50** (2.8 mg, 39% yield) as a colorless oil: $[\alpha]_D^{25}$ +10.9 (c 0.09, CHCl₃); $\Delta\epsilon$ = –2.69 (209 nm, isooctane); ¹H NMR (400 MHz, CDCl₃) δ 1.39 (s, 9H), 2.45 (q, *J* = 6.7 Hz, 1H), 2.67 (dd, *J* = 13.2, 8.3 Hz, 1H), 2.92 (d, *J* = 6.8 Hz, 2H), 3.55–3.76 (m, 3H), 3.64 (s, 3H), 4.47 (br, 1H), 4.62 (br, 1H), 4.64 (dd, *J* = 35.4, 10.0 Hz, 1H), 4.68 (br, 1H), 7.10–7.32 (m, 10H); ¹³C NMR (100 MHz, CDCl₃) δ 29.6, 32.9, 36.1, 38.3, 41.0, 51.2, 52.4, 79.8, 103.5, 126.5, 126.8, 128.1, 128.2, 128.6, 129.1, 135.5, 137.5, 153.8, 161.1, 172.0; HRMS (FAB), *m/z* calcd for C₂₆H₃₃FNO₄S (MH⁺) 474.2114, found 474.2109.

Methyl (2*S*,5*R*,3*Z*)-2-Benzylsulfanylmethyl-5-[*N*-(*tert*-butoxycarbonyl)amino]-4-fluoro-6-phenylhex-3-enoate (52). By use of a procedure similar to that described for the preparation of the ester **50**, the β -lactone **48** (5 mg, 0.0149 mmol) was converted into the title compound **52** (2.6 mg, 37% yield) as a colorless oil: $[\alpha]_D^{25}$ +68.5 (c 0.15, CHCl₃); $\Delta\epsilon$ = +1.31 (217 nm, isooctane); ¹H NMR (400 MHz, CDCl₃) δ 1.40 (s, 9H), 2.33 (dd, *J* = 13.4, 6.1 Hz, 1H), 2.52–2.61 (m, 1H), 2.87–2.94 (m, 2H), 3.59–3.70 (m, 3H), 3.68 (s, 3H), 4.45 (br, 1H), 4.64 (dd, *J* = 35.5, 9.9 Hz, 1H), 4.68 (br, 1H), 6.99–7.34 (m, 10H); ¹³C NMR (100 MHz, CDCl₃) δ 29.6, 31.9, 36.1, 38.5, 41.5, 52.0, 52.4, 79.9, 103.6, 126.6, 126.8, 128.1, 128.2, 128.6, 129.1, 135.5, 137.5, 154.0, 161.1, 172.0; HRMS (FAB), *m/z* calcd for C₂₆H₃₃FNO₄S (MH⁺) 474.2114, found 474.2121.

Acknowledgment. We thank Dr. Terrence R. Burke, Jr. (NCI, NIH, Frederick, MD 21702-1201) for proofing the manuscript. This research was supported in part by the 21st Century COE Program Knowledge Infrastructure for Genome Science, a Grant-in-Aid for Scientific Research from the Ministry of Education, Culture, Sports, Science and Technology, Japan, the Japan Society for the Promotion of Science, and the Japan Health Science Foundation.

Supporting Information Available: Experimental procedure for compounds in the b-series of Schemes 1 and 2; ORTEP diagrams for **31** and **36** and their CIF files; copies of ¹H NMR spectra of compounds **16a**, **16b**, **23a**, **23b**, **30**, and **47–52**; and copies of CD spectra of compounds **49–52**. This material is available free of charge via the Internet at <http://pubs.acs.org>.

JO035709D

CXCR4 antagonist inhibits stromal cell-derived factor 1-induced migration and invasion of human pancreatic cancer

Tomohiko Mori,¹ Ryuichiro Doi,¹ Masayuki Koizumi,¹ Eiji Toyoda,¹ Daisuke Ito,¹ Kazuhiro Kami,¹ Toshihiko Masui,¹ Koji Fujimoto,¹ Hirokazu Tamamura,² Kenichi Hiramatsu,² Nobutaka Fujii,² and Masayuki Imamura¹

¹ Department of Surgery and Surgical Basic Science and
² Department of Bioorganic Medicinal Chemistry, Graduate School of Pharmaceutical Sciences, Kyoto University, Kyoto, Japan

Abstract

The stromal cell-derived factor-1 (SDF-1)/CXCR4 system is implicated in various instances of cell migration in mammals, including the migration of lymphocytes and the formation of metastases. We have recently synthesized a potent novel CXCR4 antagonist, TN14003. The purpose of this study was to investigate the role of SDF-1/CXCR4 axis in the pancreatic cancer metastasis via cell migration and invasion, and the inhibitory effect of TN14003 on pancreatic cancer cell metastasis. The expression of CXCR4 was detected in six pancreatic cancer cell lines by Western blotting and immunocytochemistry. In migration and invasion assays, SDF-1 stimulated both migration and invasion of cancer cells in a dose-dependent manner. The maximal effect of SDF-1 was observed at 100 ng/ml. SDF-1-induced migration and invasion of cancer cells were completely blocked by 100 nM TN14003. The stimulatory effect of SDF-1 on cancer migration and the inhibitory effect of TN14003 were mediated via the alteration in phosphorylation of mitogen-activated protein kinases. Treatment of cancer cells with 100 ng/ml SDF-1 resulted in a significant increase of actin polymerization, which was reduced by 100 nM TN14003. SDF-1 enhanced cancer cell adhesion to laminin, which was not reversed by TN14003. Taken together, SDF-1/CXCR4 axis is involved in pancreatic cancer metastasis through migration and invasion. The small molecule antagonists against CXCR4 such as TN14003 might be an effective anti-metastatic agent for pancreatic cancer. [Mol Cancer Ther. 2004;3(1):29–37]

Received 8/11/03; revised 10/13/03; accepted 10/16/03.

Grant support: Grant-in-Aid for Scientific Research (#15390395) from the Ministry of Education, Culture, Sports, Science and Technology of Japan.

The costs of publication of this article were defrayed in part by the payment of page charges. This article must therefore be hereby marked advertisement in accordance with 18 U.S.C. Section 1734 solely to indicate this fact.

Note: T. Mori and R. Doi contributed equally.

Requests for Reprints: Ryuichiro Doi, Department of Surgery and Surgical Basic Science, Kyoto University, 54-Shogoin Kawara-cho, Sakyo, Kyoto 606-8507, Japan. Phone: 81-75-751-3671; Fax: 81-75-751-3219. E-mail: doir@kuhp.kyoto-u.ac.jp

Introduction

The chemokines are a family of low molecular weight cytokines that mediate the chemical effect on target cells through seven-transmembrane G-protein-coupled receptors (1–4). Stromal cell-derived factor-1 (SDF-1), which was initially cloned by Tashiro *et al.* (5), is a member of the CXCL subfamily of chemokines and interacts with the seven-transmembrane G-protein-coupled receptor CXCR4, an exclusive receptor for SDF-1 (6, 7). Later, SDF-1 was identified as a growth factor for B-cell progenitors and also a chemotactic factor for T cells and monocytes relevant to B-cell lymphopoiesis and bone marrow myelopoiesis (6, 8, 9). Furthermore, SDF-1 was found to play a critical role in directed cell migration (6, 10) and embryonic development (8, 11, 12). Most importantly, the function of a subset of chemokine receptors as co-receptors for the entry of HIV-1 was clarified. CXCR4 and a CC-chemokine receptor, CCR5, represent major co-receptors for the entry of T-cell line-tropic HIV-1 (X4-HIV-1) and macrophage-tropic HIV-1 (R5-HIV-1), respectively (13, 14).

Recently, several studies have been conducted to detect the expression of CXCR4 and SDF-1 in solid tumors. The results are not uniform, and the relevance to cancer progression and tumor angiogenesis is unclear (15–17). In breast cancer, the SDF-1/CXCR4 system has been implicated in the formation of metastasis (18). Before this, we found that SDF-1 mRNA expression is detected in pancreatic cancer tissues, but is not detected in pancreatic cancer cell lines, whereas CXCR4 mRNA expression is detected in both pancreatic cancer tissues and cancer cell lines (19). To date, however, the role of interaction between SDF-1 and CXCR4 in pancreatic cancer progression has not been defined.

The specific ligands for these receptors are able to inhibit HIV infection (20–23). As for the malignant solid tumors, neutralizing the interactions of SDF-1/CXCR4 by administration of an antibody to CXCR4 significantly impairs metastasis of breast cancer cells to regional lymph node and lung in the animal model. For this reason, efforts have focused on developing a specific antagonist for chemokine receptors.

A CXCR4 antagonist, T22, was previously discovered as an anti-HIV peptide based on chemical conversions of horseshoe crab self-defense peptides, tachyplesins and polyphemusins (24). On the basis of T22 structure, we reported the synthesis of a novel CXCR4 inhibitor, T140 (25). T140 strongly antagonizes CXCR4 function, though it is not stable in serum due to the cleavage of COOH-terminal Arg¹⁴. Consequently, we reported that the COOH-terminal amidation and the double-L-citrulline (Cit)-scanning of T140 led to development of a novel effective CXCR4 inhibitor, TN14003, which possesses high selectivity index and complete stability in serum, without significant change in the secondary structure. (25). In this

study, we investigated the role of SDF-1/CXCR4 axis in human pancreatic cancer cells, and tested the inhibitory effect of the novel CXCR4 inhibitor, TN14003, on *in vitro* cell functions that are relevant to metastasis.

Materials and Methods

SDF-1 and TN14003

We synthesized TN14003 and SDF-1 as described previously (25). TN14003 shows the highest level of anti-HIV activity and antagonism of target cell entry by X4-HIV-1 among all the CXCR4 antagonists that have been reported to date, and possesses complete stability in serum (25).

Reagents and Antibodies

The following antibodies and reagents were purchased: An affinity-purified goat anti-CXCR4 polyclonal antibody (sc-6190, Santa Cruz Biotechnology, Santa Cruz, CA); a mouse anti-human CXCR4 monoclonal antibody (MAB172, R&D Systems, Minneapolis, MN); anti-phospho-p44/42 mitogen-activated protein (MAP) kinase antibody (#9106, Cell Signaling Technology, Beverly, MA); anti-p44/42 MAP kinase antibody (#9102, Cell Signaling Technology); PD98059 (Calbiochem, San Diego, CA); Cy3-conjugated Affinipure goat anti-mouse IgG (Jackson ImmunoResearch Laboratories, West Grove, PA); and rhodamine-phalloidin (R-415, Molecular Probes, Eugene, OR).

Cell Line and Culture Conditions

Human pancreatic cancer cell lines (CFPAC-1, Capan-2, AsPC-1, PANC-1, BxPC-3, and SUIT-2) were maintained in the following media at 37°C in a humid atmosphere of 5% CO₂/95% air. CFPAC-1 cells were cultured in Iscove's modified Dulbecco's medium with 10% fetal bovine serum (FBS). PANC-1 cells were cultured in DMEM with 10% FBS. BxPC-1 cells, Capan-2 cells, AsPC-1 cells, and SUIT-2 cells were cultured in RPMI 1640 with 10% FBS. Each medium contained 100 units/ml penicillin and 0.1 mg/ml streptomycin.

Expression of CXCR4 in Pancreatic Cancer Cells

Serum-starved subconfluent cells were harvested, washed in cold PBS, and lysed in ice-cold lysis buffer [10 mM PBS (pH 7.4), 1% NP40, 0.5% sodium deoxycholate, 0.1% SDS, 5 mM EDTA] supplemented with 1% phenylmethylsulfonyl fluoride and 0.02 mg/ml gabexate mesilate, a synthetic protease inhibitor (FOY, Ono Pharmaceutical, Osaka, Japan) for 30 min at 4°C. The lysate was homogenized and centrifuged at 15,000 rpm for 30 min at 4°C to remove debris, and the protein concentration was measured using a BCA protein assay kit (Pierce, Rockford, IL). The extracted protein was subjected to Western blotting, as previously described (26). Equal amounts of protein were loaded onto 10% SDS-polyacrylamide gels and the proteins were transferred to polyvinylidene difluoride membrane (Bio-Rad, Richmond, CA). Blots were blocked at 4°C overnight with 5% (w/v) nonfat milk in TTBS buffer (10 mM Tris-HCl, 150 mM NaCl, 0.5% Tween 20). The blots were incubated for 1 h at room temperature with the primary antibody against CXCR4 (sc-6190, Santa Cruz Biotechnology) diluted at 1:100 with TTBS. The blots were incubated for 1 h with a second antibody (200 ng/ml alkaline

phosphatase-conjugated anti-goat IgG, Pierce). Immunoreactive proteins were visualized using alkaline phosphatase solution supplemented with 100 mM Tris-HCl, 100 mM HCl, 5 mM MgCl₂, 0.03% nitroblue tetrazolium, and 0.017% 5-bromo-indolylphosphate P-toluidine salt.

Immunocytochemistry

Pancreatic cancer cells were seeded on coverslips and incubated for 24 h at 37°C in a humid atmosphere of 5% CO₂/95% air. The coverslips with cells were then fixed with 4% paraformaldehyde in PBS for 10 min, washed with PBS, permeabilized in 1% Triton X-100 in PBS for 15 min, washed, and blocked with TTBS with 1% BSA. For CXCR4 staining, fixed and permeabilized cells were incubated with mouse anti-human CXCR4 monoclonal antibody (MAB172, R&D Systems) diluted in 1% BSA-TTBS (0.01 mg/ml) for 2 h at 37°C, and rinsed 3 times with TTBS, and then incubated for 30 min with secondary antibody (Cy3-conjugated Affinipure goat anti-mouse IgG, Jackson ImmunoResearch) diluted in 1% BSA-TTBS (1:100). After the final wash, coverslips were mounted on the slide-glass using 50% solution of glycerol in PBS. The cells were examined under a fluorescence microscope (Olympus, Tokyo, Japan).

In Vitro Proliferation Assay

Pancreatic cancer cells (AsPC-1, PANC-1, and SUIT-2) were seeded at a density of 5000 cells per well into 96-well plates in culture medium containing 10% FBS. After 24 h, the cultures were washed and refed with medium alone (control) or with medium containing SDF-1 or TN14003 at various concentrations. After 3 days, the number of viable cells was counted using Cell Counting Kit 8 (Dojindo Co., Kumamoto, Japan) according to the manufacturer's instructions. The assay reagent is a tetrazolium compound (WST-x8) that is reduced by live cells into a colored formazan product measured at 450 nm. The quantity of formazan product measured at 450 nm is directly proportional to the number of live cells in the culture. The experiments were repeated in triplicate wells.

In Vitro Migration Assays

Migration of cancer cells was assayed using 6.5-mm-diameter chambers with 8-μm pore filters (Transwell, 24-well cell culture, Costar, Boston, MA). Pancreatic cancer cells were suspended at 2 × 10⁵ cells/ml in serum-free media, and then 0.2 ml cell suspension was added to the upper chamber. Then, 0.5 ml serum-free media with various concentrations of SDF-1 was added to the lower chamber. In another set of experiments, 0.5 ml serum-free media with 100 ng/ml of SDF-1 (fixed concentration) plus various concentrations of TN14003 was added to the lower chamber. The chambers were incubated for 12 h at 37°C in a humid atmosphere of 5% CO₂/95% air. After incubation, the filters were fixed and stained with Diff-Quick reagent (Dade Behring, Dugan, Switzerland). The upper surface of the filters was scraped twice with cotton swabs to remove non-migrating cells. The experiments were repeated in triplicate wells, and the number of migrating cells in five high-power fields per filter was counted microscopically at ×400 magnification. Because the background migration without SDF-1 varied among experiments, data were normalized as the migration

index: the number of migrating cells in an experimental chamber/the number of migrating cells in control chamber without SDF-1. In another experiment, cells were pretreated with 30 μ M PD98059 (Calbiochem), a MEK1 inhibitor, before SDF-1 treatment.

In Vitro Invasion Assays

Invasion of cancer cells was assayed using a Biocoat Matrigel invasion chamber (Becton Dickinson, Bedford, MA), which consists of an 8- μ m pore size polyethylene terephthalate (PET) membrane that has been overlaid with Matrigel (basement membrane matrix). PANC-1, SUIT-2, or AsPC-1 cells were suspended at 2×10^5 cells/ml in serum-free media, and then 0.2 ml cell suspension was added to the upper chamber. Next, 0.5 ml serum-free media with 100 ng/ml of SDF-1 (fixed concentration) plus various concentrations of TN14003 was added to the lower chamber. The chambers were incubated for 12 h at 37°C in a humid atmosphere of 5% CO₂/95% air. After incubation, the filters were fixed and stained with Diff-Quick reagent (Dade Behring). The upper surface of the filters was scraped twice with cotton swabs to remove non-invading cells. The experiments were repeated in triplicate wells, and the number of invading cells in five high-power fields per filter was counted microscopically at $\times 400$ magnification. The data were processed by the method described in migration assay.

Detection of p44/42 MAP Kinases in Pancreatic Cancer Cells

Cells were put in DMEM containing low levels of BSA (0.5%) to render the cells quiescent. Then cells were incubated with 100 ng/ml SDF-1 or 100 ng/ml SDF-1 plus 100 nM TN14003 for 5 min to 1 h at 37°C. In another setting, PANC-1 cells were preincubated for 1 h at 37°C with 10 μ M PD98059 (Calbiochem), a MEK1 inhibitor, before SDF-1 treatment. After treatment with SDF-1, cells were lysed for 60 min in phosphorylation-inhibitory radioimmunoprecipitation assay (RIPA) buffer containing 50 mM HEPES (pH 7.0), 250 mM NaCl, 0.1% NP40, 1 mM phenylmethylsulfonyl fluoride, and 20 μ g/ml gabexate mesilate, then the lysate was sonicated for 10 s. Total extracts were cleaned by centrifugation at 12,000 rpm for 10 min at 4°C, and the supernatants were collected. Protein concentrations were measured using a protein assay kit (Tonein-TP, Otsuka Pharmaceutical, Tokyo, Japan). The lysates were resuspended in 1 volume of the gel loading buffer that contained 50 mM Tris-HCl (pH 6.7), 4% SDS, 0.02% bromophenol blue, 20% glycerol, and 4% 2-mercaptoethanol, and then boiled at 95°C for 90 s. The extracted protein was subjected to Western blotting, as previously described (26). In brief, 30- μ g aliquots of protein were size-fractionated to a single dimension by SDS-PAGE (12% gels) and transblotted to a 0.45- μ m polyvinylidene difluoride membrane (Bio-Rad) in a semidry electroblot apparatus (Bio-Rad). The blots were then washed 3 times with TTBS buffer and incubated for 2 h at room temperature in the first antibody solution containing anti-phospho-p44/42 MAP kinase antibody (#9106, Cell Signaling Technology). After three washings in TTBS buffer, the blots were incubated for 1 h at room

temperature with horseradish peroxidase-conjugated secondary antibody. After three washings in TTBS buffer, membranes were treated with enhanced chemiluminescence reagents (Amersham Life Sciences, Amersham, United Kingdom) according to the manufacturer's protocol. Membranes were exposed to X-ray film for 50 s. Protein expression was measured by a densito-analyzer system (AE-6920M, ATTO Corporation, Tokyo Japan). After stripping and blocking, the same blots were re-probed with anti-p44/42 MAP kinase antibody (#9102, Cell Signaling Technology) to measure total MAP kinase.

Actin Cytoskeleton

Pancreatic cancer cells were seeded on coverslips and incubated for 24 h at 37°C in a humid atmosphere of 5% CO₂/95% air. Then the cells were incubated in serum-free medium containing 0.1% BSA with 100 ng/ml SDF-1 or with 100 ng/ml SDF-1 plus 100 nM TN14003 for 1 h at 37°C. The coverslips with cells were then fixed with 4% paraformaldehyde in PBS for 10 min, washed with PBS, permeabilized in 1% Triton X-100 in PBS for 15 min, washed, and blocked with TTBS with 1% BSA. For visualization of filamentous actin, the cells were exposed to rhodamine-phalloidin for 30 min at 37°C and washed with TTBS. After final wash, coverslips were mounted on the slide-glass using 50% solution of glycerol in PBS. The cells were examined under a fluorescence microscope (Olympus).

Adhesion Assay

The adhesion of pancreatic cancer cells to the elements of extracellular matrix (ECM) was evaluated. Pancreatic cancer cells were grown to subconfluent state and then harvested by 0.25% trypsin/EDTA (Invitrogen Corp., Carlsbad, CA) in 1 min. Cells were preincubated with SDF-1 or with SDF-1 plus TN14003. The same volume of vehicle was added to cells as a control. Preincubated cells were plated onto a 96-well microplate which was precoated with various kinds of ECM elements, that is, 0.01 mg/ml plasma fibronectin, 0.01 mg/ml vitronectin or Matrigel, or 96-well Microtest Plate (BioCoat, Becton-Dickinson Japan, Tokyo, Japan) precoated with collagen I, collagen IV, or laminin. Then the cells were incubated for 3 h at 37°C in 5% CO₂/95% air to allow cell attachment. Cells were washed gently with PBS 3 times to remove detached cells. The number of adherent cells was measured by WST method using Cell Counting Kit 8 (Dojindo). Experiments were repeated 3 times in triplicate wells.

Statistical Analysis

Statistical comparisons were performed by a two-way ANOVA for repeated measures, followed by a post hoc Turkey test, or Student's two-tailed *t* test. *P* < 0.05 was considered to be significant.

Results

Expression of CXCR4 in Pancreatic Cancer Cells

The expression of CXCR4 in six pancreatic cancer cell lines (CFPAC-1, Capan-2, AsPC-1, PANC-1, BxPC-3, and SUIT-2) was examined. Western blot analysis demonstrated definite expression of immunoreactive CXCR4 protein in

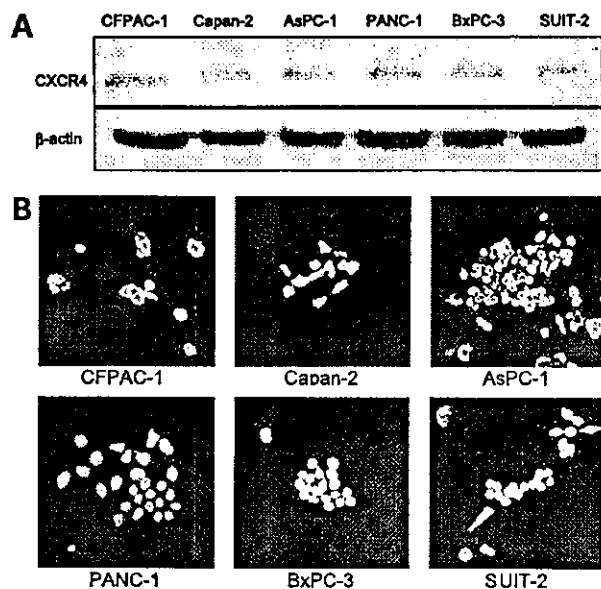


Figure 1. Expression of CXCR4 in pancreatic cancer cells. **A**, CXCR4 was detected in pancreatic cancer cell lines by Western blot. The CXCR4 expression level was similar among six cell lines (CFPAC-1, Capan-2, AsPC-1, PANC-1, BxPC-3, and SUIT-2). **B**, CXCR4 was detected by immunocytochemistry in pancreatic cancer cells. Immunoreactive CXCR4 was located in the cytosol and membrane of the pancreatic cancer cells.

all pancreatic cancer cell lines. The strength of CXCR4 expression was similar among the six cell lines (Fig. 1A). Immunocytochemistry demonstrated the expression of CXCR4 in all pancreatic cancer cells (Fig. 1B).

Effect of SDF-1 on Pancreatic Cancer Cell Proliferation

The effect of SDF-1 on cell proliferation was examined in pancreatic cancer cell lines (AsPC-1, PANC-1, and SUIT-2). After incubation for 72 h, the cell proliferation was not significantly changed by SDF-1 at concentrations from 50 to 200 ng/ml (Fig. 2A).

Effect of TN14003 on Pancreatic Cancer Cell Proliferation

We found that the 50% effective concentration (EC_{50}) of TN14003 against HIV-induced cytopathogenicity in MT-4 cells was 0.6 nM, and the 50% cytotoxic concentration (CC_{50}) of TN14003 against human peripheral blood mononuclear cells (PBMCs) was 410 μ M (25). Then, the selectivity index ($SI = [CC_{50}/EC_{50}]$) of TN14003 in this system was 680,000, and the complete inhibitory concentration of TN14003 was conjectured between 20 and 80 nM from these data. Thus, the effect of TN14003 at concentrations up to 10 μ M was tested in terms of proliferation of pancreatic cancer cells (AsPC-1, PANC-1, and SUIT-2). TN14003 showed no inhibitory effect on cell proliferation at concentrations up to 100 nM (Fig. 2B). The cell proliferation was slightly suppressed at 1 and 10 μ M, but the suppression was not statistically significant for PANC-1 and SUIT-2. TN14003 at 10 μ M suppressed the proliferation of AsPC-1 (Fig. 2B). Therefore, the following experiments were performed by using TN14003 at concentrations less than 10 μ M.

Effect of TN14003 on SDF-1-Induced Migration and Invasion of Pancreatic Cancer Cells

SDF-1 stimulated the migration of pancreatic cancer cells (Fig. 3). Maximal effect was observed at 100 ng/ml of SDF-1 in all pancreatic cancer cell lines, and maximal migration indices were $214 \pm 27\%$ in PANC-1 cells, $191 \pm 35\%$ in AsPC-1 cells, and $159 \pm 17\%$ in SUIT-2 cells, respectively. Supramaximal suppression was observed at concentrations over 100 ng/ml in this system. Next, the inhibitory effect of TN14003 on SDF-1-induced migration was tested. The migration induced by SDF-1 at 100 ng/ml was inhibited by TN14003 in PANC-1, AsPC-1, and SUIT-2 cells, and was completely blocked by TN14003 at 100 nM (Fig. 4).

The effects of SDF-1 and TN14003 on cancer cell invasion were tested. SDF-1 at 100 ng/ml induced maximal effect and the maximal invasion indices were $150 \pm 14\%$ in PANC-1 cells, $180 \pm 15\%$ in AsPC-1 cells, and $168 \pm 8\%$ in SUIT-2 cells. The invasion induced by SDF-1 at 100 ng/ml was inhibited by TN14003 in all cancer cells, and was completely blocked by TN14003 at 100 nM (Fig. 5) Meanwhile, T22, a lead compound for TN14003 (27), did not completely block the migration and invasion at the same concentration.

Effect of SDF-1 and TN14003 on Actin Cytoskeleton of PANC-1 Cells

Serum-starved cells displayed low levels of F-actin as judged by phalloidin staining (Fig. 6A). After treatment with SDF-1 at 100 ng/ml for 1 h, PANC-1 cells showed intense F-actin staining in the periphery of the cells, distinct pseudopodia formation, and stress fibers (actin polymerization, Fig. 6B). Addition of TN14003 at 100 nM eradicated the SDF-1-induced actin polymerization (Fig. 6C). The cells that express actin polymerization were counted microscopically in five high-power fields at $\times 400$ magnification. The ratio of cells with actin polymerization was $41 \pm 8\%$ ($n = 3$) in control medium, $75 \pm 7\%$ ($n = 3$) in cells with SDF-1, and $47 \pm 7\%$ ($n = 3$) in cells with SDF-1 plus TN14003.

Involvement of p44/42 MAP Kinases in Pancreatic Cancer Cell Mobility

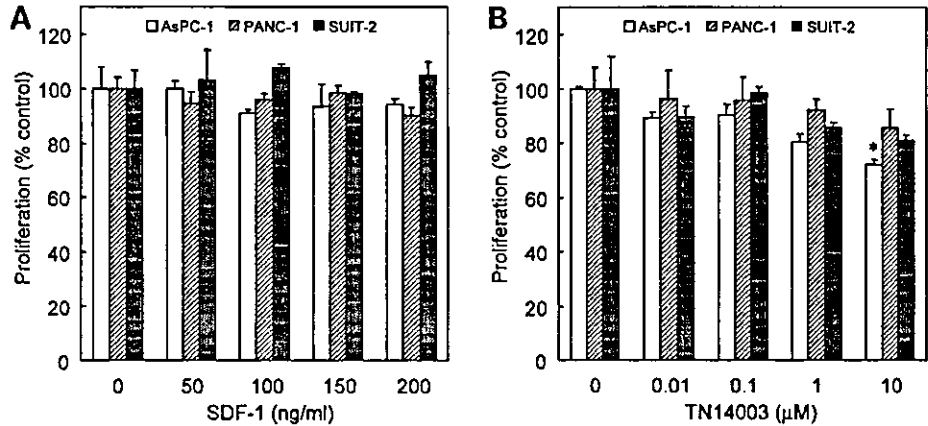
To explain the mechanism by which TN14003 inhibited the migration and invasion of pancreatic cancer cells, we next investigated the involvement of p44/42 MAP kinases. When PANC-1 cells were incubated with 100 ng/ml SDF-1, the phosphorylated p44/42 MAP kinase (Erk1/2) was transiently increased peaking at 10 min following addition of SDF-1 and dropping back to baseline thereafter (Fig. 7A). An addition of TN14003 abolished the SDF-1-induced phosphorylation of p44/42 MAP kinase.

Therefore, we next investigated whether the phospho-p44/42 MAP kinase is involved in the cancer cell mobility. Pretreatment of PANC-1 cells with PD98059 resulted in a suppression of SDF-1-induced phosphorylation of p44/42 MAP kinase (Fig. 7B). At the same time, pretreatment of PANC-1 cells with PD98059 abolished the increased migration induced by SDF-1 (Fig. 7C).

Cell Adhesion Assay

The effects of SDF-1 on pancreatic cancer cell adhesion to the elements of ECM were tested. The number of adherent

Figure 2. Effect of SDF-1 and TN14003 on the proliferation of pancreatic cancer cells. **A**, pancreatic cancer cells (*AsPC-1*, *PANC-1*, and *SUIT-2*) were incubated in the presence of SDF-1 at various concentrations (0–200 ng/ml). After 72 h, the number of viable cells was counted. *Columns*, mean of triplicate samples from three independent experiments; *bars*, SE. **B**, pancreatic cancer cells (*AsPC-1*, *PANC-1*, and *SUIT-2*) were incubated in the presence of TN14003 at various concentrations (0–10 μ M). After 72 h, the number of viable cells was counted. *Columns*, mean of triplicate samples from three independent experiments; *bars*, SE. *, $P < 0.05$ compared with control.



cells to fibronectin, vitronectin, and collagen I was not changed by SDF-1 (Fig. 8, A–C). In contrast, the number of adherent cells to Matrigel was increased by SDF-1 (Fig. 8D). Matrigel is a solubilized basement membrane matrix extracted from the Engelbreth-Holm-Swarm mouse tumor, and is composed of collagen IV, laminin, and other elements. Therefore, we tested the effects of SDF-1 on cell adhesion to collagen IV and laminin-coated plate. SDF-1 induced increase of pancreatic cancer cell adhesion to laminin but not to collagen IV (Fig. 8, E and F). The increasing effect of SDF-1 on pancreatic cancer cell adhesion to laminin was not reversed by an addition of TN14003 (data not shown).

Discussion

In this report, we investigated the expression of CXCR4 in pancreatic cancer cell lines and determined the effects of

its ligand, SDF-1. We showed that all the six human pancreatic cancer cell lines express the CXCR4 receptors by Western blotting and immunocytochemistry. Recent reports have demonstrated that CXCR4 receptors are expressed in most small cell lung cancer cells (16), ovarian cancer cells (28), and melanoma cells (29). In contrast, CXCR4 mRNA expression in colon, esophageal, or gastric cancers were not different from that of non-cancerous tissues, and CXCR4 mRNA expression in hepatocellular carcinoma were reduced when compared to non-cancerous liver tissue (17, 30). We found that CXCR4 mRNA was detected in both pancreatic cancer tissues and cancer cell lines, whereas SDF-1 mRNA expression was detected in all pancreatic cancer tissues but was not detected in pancreatic cancer cell lines (19). These findings indicate that the paracrine mechanism may be involved in the SDF-1/CXCR4 ligand receptor system in those solid tumors that express CXCR4 receptors. The transcription

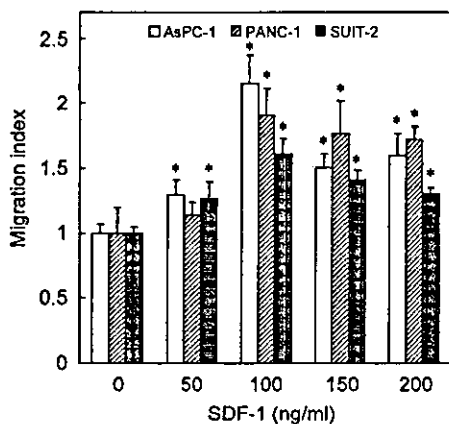


Figure 3. Effect of SDF-1 on migration of pancreatic cancer cells. Migration of pancreatic cancer cells was tested as described in the Materials and Methods. SDF-1 stimulated the migration of pancreatic cancer cells. Maximal effect was observed at 100 ng/ml of SDF-1, and the supra-maximal suppression was observed at concentrations over 100 ng/ml. *, $P < 0.05$ compared with control.

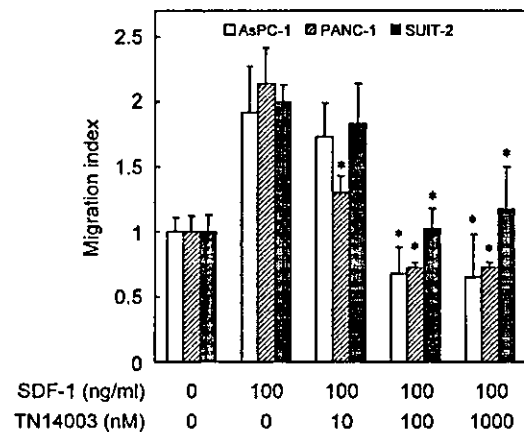


Figure 4. Effect of TN14003 on SDF-1-stimulated migration of pancreatic cancer cells. Pancreatic cancer cells were stimulated by SDF-1 at 100 ng/ml and various concentrations of TN14003. The SDF-1-stimulated migration was inhibited by TN14003 and was completely eradicated by TN14003 at 100 nM. *Columns*, mean of three separate experiments in triplicate wells; *bars*, SE. *, $P < 0.05$ compared with 100 ng/ml SDF-1.

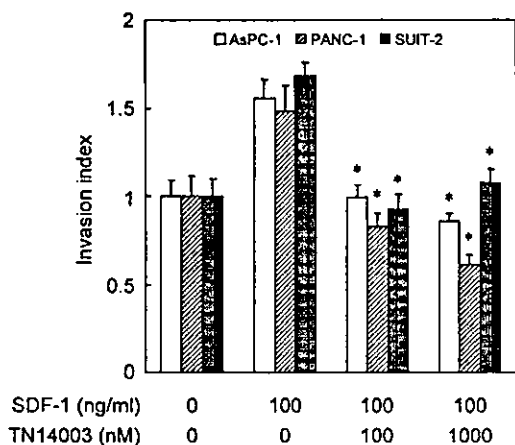


Figure 5. Effect of TN14003 on SDF-1-stimulated invasion of pancreatic cancer cells. Pancreatic cancer cells were stimulated by SDF-1 at 100 ng/ml and various concentrations of TN14003. The SDF-1-stimulated invasion was inhibited by TN14003 and was completely eradicated by TN14003 at 100 nM. Columns, mean of three separate experiments in triplicate wells; bars, SE. *, $P < 0.05$ compared with 100 ng/ml SDF-1.

factors that regulate CXCR4 expression are currently unknown. Recently, it has been reported that NF- κ B regulates the motility of cancer cells by directly up-regulating the expression of CXCR4 (31).

In pancreatic cancer cell lines, we showed that SDF-1 had no direct effect on cell proliferation. Our result is in accordance with the recent study which showed that SDF-1 had no proliferative effects on rhabdomyosarcoma (32). It also agrees with a report demonstrating lack of a proliferative effect by SDF-1 on colony-forming units-megakaryocyte (CFU-MK) (33) or lymphohematopoietic cells (34). In contrast, recent reports demonstrated that SDF-1 stimulates proliferation of small cell lung cancer cells (NCI-H69) in the presence of serum (16), that SDF-1 acts together with thrombopoietin to enhance the development of CFU-MK in a murine model (35) and that SDF-1 at low doses enhances the proliferation of peripheral blood CD34⁺ cells (36). In addition, antisense CXCR4 overexpression in

glioblastoma cells caused inhibition of cell proliferation, suggesting that SDF-1/CXCR4 system is involved in cell proliferation in glioblastoma cell lines as well (15, 37). We suggest that these differences may be due to the different culture system or to the different target cells.

Although we did not find any effect of SDF-1 on proliferation of pancreatic cancer cells, we found that SDF-1 stimulates cell metastasis and invasive behavior. In migration assay by Transwell chamber, SDF-1 significantly increased migration of pancreatic cancer cells. The cancer cells responded to SDF-1 in a similar manner, and maximal effect by SDF-1 was observed at 100 ng/ml. Invasion assay by Matrigel-coated invasion chamber also showed that SDF-1 significantly stimulated invasion of pancreatic cancer cell. Previous reports similarly showed that invasion through Matrigel was stimulated by SDF-1 in CXCR4-expressing ovarian cancer cells (38), prostate cancer cells (39), and myeloma cells (40). Video microscopic examination revealed that SDF-1 stimulated the motility of small cell lung cancer cells (16).

It has recently been reported that CXCR4 was highly expressed in malignant but not normal breast tissue, and that its ligand, SDF-1, is expressed in those organs where breast cancer metastasis is frequently found (bone marrow, lymph node, lung, and liver) (18). Furthermore, neutralizing the interactions of SDF-1/CXCR4 by administration of an antibody to CXCR4 significantly impairs metastasis of breast cancer cells to regional lymph node and lung in their breast cancer metastasis model. These reports, taken together with the current results, indicate that SDF-1/CXCR4 interaction may be generally important for the metastasis of solid tumors that express CXCR4.

In tumor cells, high levels of actin polymerization are required for the formation of stress fiber and pseudopodia, which in turn are implicated in the enhancement of cell migration and invasion. We showed that the treatment of pancreatic cancer cells with SDF-1 resulted in a dramatic increase in actin polymerization, which is needed for the invasion of malignant cells into tissues and for efficient metastasis. These findings suggest that SDF-1/CXCR4 ligand receptor system plays an important role in invasion as well as metastasis in pancreatic cancer.

Since CXCR4 was identified as a co-receptor for the entry of T-cell line-tropic (T-tropic) HIV-1 (13, 14), development



Figure 6. Effect of SDF-1 and TN14003 on actin cytoskeleton in PANC-1 cells. PANC-1 cells were incubated for 1 h in serum-free medium containing 0.1% BSA with 100 ng/ml SDF-1 or 100 ng/ml SDF-1 plus 100 nM TN14003. Subsequently, cells were stained with rhodamine-phalloidin to visualize F-actin. Untreated cells (A), cells treated with SDF-1 (B), and cells treated with SDF-1 and TN14003 (C).

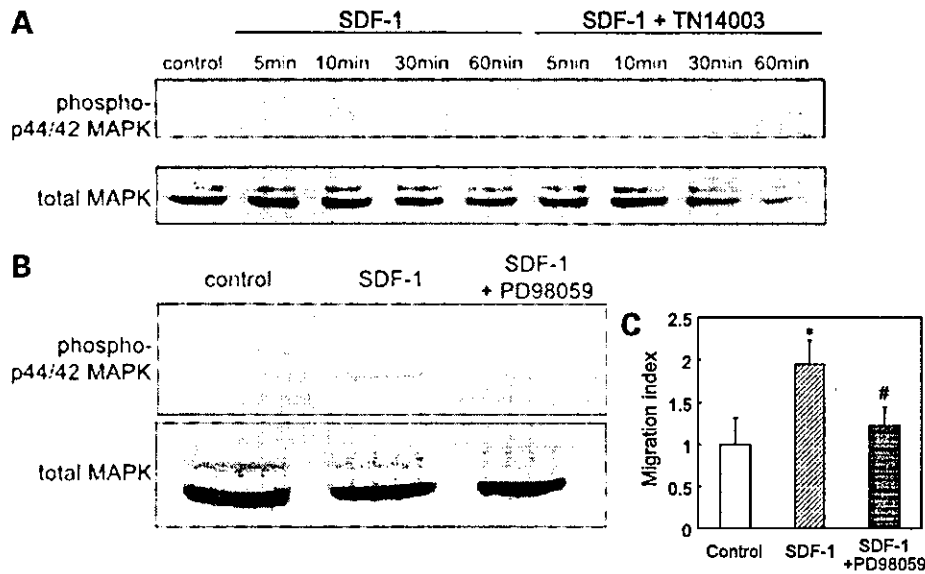


Figure 7. Effect of TN14003 on SDF-1-induced phosphorylation of p44/42 MAP kinase (Erk 1 and 2) in pancreatic cancer cells. **A**, PANC-1 cells were treated with SDF-1 alone or SDF-1 plus TN14003. Cells were harvested at 5, 10, 30, and 60 min, and phospho-p44/42 MAP kinase and total MAP kinase were detected as described. SDF-1 induced the maximal level of phosphorylation of p44/42 MAP kinase at 10 min. The addition of TN14003 eradicated the SDF-1-induced phospho-p44/42 MAP kinase. **B**, PANC-1 cells were treated with SDF-1 alone or SDF-1 plus PD98059. Cells were harvested at 10 min and phospho-p44/42 MAP kinase and total MAP kinase were detected as described. Pretreatment of PANC-1 cells with PD98059 eradicated the SDF-1-induced phospho-p44/42 MAP kinase. **C**, pancreatic cancer cells were stimulated by SDF-1 at 100 ng/ml with or without pretreatment of DP98059. The SDF-1-stimulated migration was inhibited by the pretreatment of PD98059. Columns, mean of three separate experiments in triplicate wells; bars, SE. *, $P < 0.05$ compared with control. #, $P < 0.05$ compared with SDF-1.

for CXCR4 antagonists seemed an ideal approach to discover an effective anti-HIV agent. Several specific antagonists for CXCR4 have been developed to date; however, there was no effective agent that satisfied both pharmacological and clinical requirements. The CXCR4 antagonist T22, which was derived from chemical conversions of horseshoe crab self-defense peptides, tachyple-

sins, and polyphemusins, had previously been discovered as an anti-HIV peptide (24).

On the basis of the structure-activity relationship study (SAR) of T22, we previously synthesized a more effective analogue, T140 (27). This agent showed the highest level of anti-HIV activity and antagonism of target cell entry by X4-HIV-1 among all the CXCR4 antagonists that have been

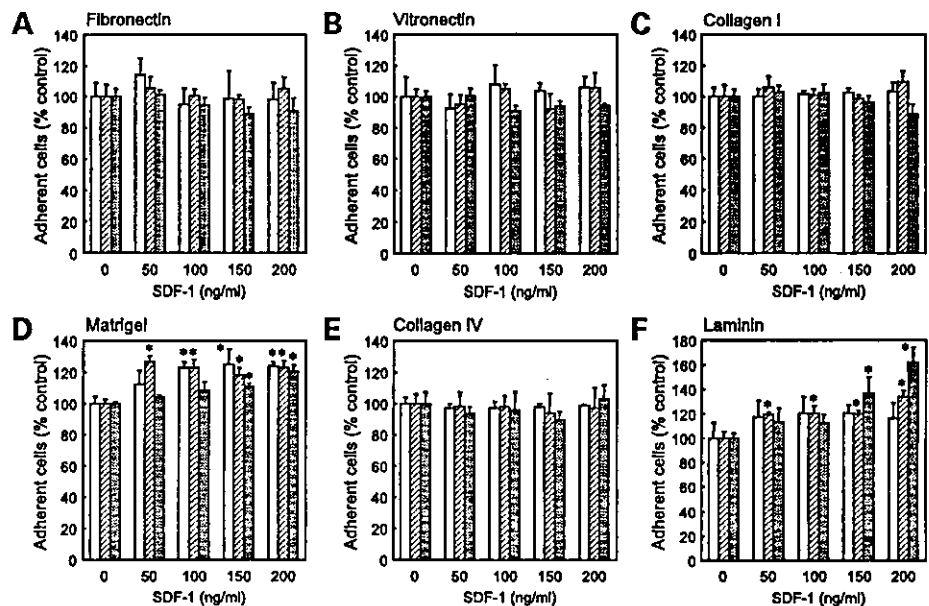


Figure 8. The effects of SDF-1 on pancreatic cancer cell adhesion to the elements of extracellular matrix. The number of adherent cells to fibronectin (**A**), vitronectin (**B**), and collagen I (**C**) was not changed by SDF-1. The number of adherent cells to Matrigel (**D**) was increased by SDF-1. The number of adherent cells to collagen IV was not changed (**E**), but that to laminin (a component of Matrigel) was increased by SDF-1 (**F**). □, AsPC-1; ▨, PANC-1; ■, SUIT-2. Columns, mean of three separate experiments; bars, SE. *, $P < 0.05$ compared with control.

reported to date. However, T140 is not stable in serum due to the cleavage of the COOH-terminal Arg, indispensable for anti-HIV activity. The COOH-terminal amidation and the double-Cit-scanning of T140 have led to development of the novel effective CXCR4 inhibitor, TN14003 (25). TN14003 has a very high selectivity index (SI [CC_{50}/EC_{50}] = 680,000) (25), that is, it showed high anti-HIV activity (EC_{50} = 0.6 nM) which was based on the protection against HIV-induced cytopathogenicity in MT-4 cells, whereas TN14003 showed low cytotoxicity (CC_{50} = 410 μ M) which was determined by the trypan blue exclusion staining method in human peripheral blood mononuclear cells. In addition, unlike T140, TN14003 possesses complete stability in serum.

Because of the high selectivity index of TN14003 for this system, we applied this agent on CXCR4-expressing human pancreatic cancer cells. We demonstrated that SDF-1-induced migration and invasion of pancreatic cancer cells were completely blocked by 100 nM TN14003. The IC_{50} of TN14003 on cancer cell migration and invasion was almost one-tenth that of T22. We demonstrated that TN14003 inhibited SDF-1-induced actin polymerization of pancreatic cancer cells. In contrast, SDF-1 stimulated adhesion of pancreatic cancer cells to laminin, one of the ECM components, but the addition of TN14003 did not reverse the effect of SDF-1. Therefore, TN14003 seems to mainly antagonize the stimulatory effect of SDF-1 on the mobility of pancreatic cancer cells. The Cit-substitution for a reduction of total cationic charges in the molecule is thought to be useful for developing effective anti-metastatic peptides, which could be a new type of anti-cancer agents against CXCR4.

In this study, we found that human pancreatic cancer cells express the chemokine receptor CXCR4, which mediate ligand-dependent cell migration and invasion *in vitro*, and that migration and invasion of pancreatic cancer cells induced by SDF-1 were completely blocked by the novel CXCR4 inhibitor TN14003. These results suggest that novel therapeutic strategies in metastasis of pancreatic cancer can be expected based on manipulation of the SDF-1 and CXCR4 ligand receptor system. This stimulative effect by SDF-1 was mediated via the MAP kinase pathway as shown by detecting increased level of phosphorylated MAP kinases, and by the fact that MAP kinase kinase inhibitor suppressed phosphorylated MAP kinases and cell mobility. These results are consistent with the previous report that showed that SDF-1 selectively activated p44/42 MAP kinase (41). The novel CXCR4 inhibitor TN14003 also suppressed SDF-1-induced phosphorylation of MAP kinases.

In conclusion, the results in this study indicate that the SDF-1/CXCR4 ligand receptor axis may play an important role in metastasis of pancreatic cancer, and that CXCR4 receptor antagonists could inhibit metastatic behavior of pancreatic cancer cells. Therefore, it is strongly suggested that TN14003 could be an effective anti-metastatic agent. Small-molecule antagonists of chemokine receptors like TN14003 may be useful in treating cancer patients.

References

1. Premack BA, Schall TJ. Chemokine receptors: gateways to inflammation and infection. *Nat Med.* 1996;2:1174–8.
2. Rollins BJ. Chemokines. *Blood.* 1997;2:909–28.
3. Mellado M, Rodriguez-Frade JM, Manes S, Martinez AC. Chemokine signaling and functional responses: the role of receptor dimerization and TK pathway activation. *Annu Rev Immunol.* 2001;2:397–421.
4. Rossi D, Zlotnik A. The biology of chemokines and their receptors. *Annu Rev Immunol.* 2000;2:217–42.
5. Tashiro K, Tada H, Heilker R, Shirozu M, Nakano T, Horjio T. Signal sequence trap: a cloning strategy for secreted proteins and type I membrane proteins. *Science.* 1993;2:600–3.
6. Bleul CC, Fuhlbrigge RC, Casasnovas JM, Aiuti A, Springer TA. A highly efficacious lymphocyte chemoattractant, stromal cell-derived factor 1 (SDF-1). *J Exp Med.* 1996;2:1101–9.
7. Wells TN, Power CA, Lusti-Narasimhan M, Hoogewerf AJ, Cooke RM, Chung CW, et al. Selectivity and antagonism of chemokine receptors. *J Leukoc Biol.* 1996;2:53–60.
8. Nagasawa T, Hirota S, Tachibana K, Takakura N, Nishikawa S, Kitamura Y, et al. Defects of B-cell lymphopoiesis and bone-marrow myelopoiesis in mice lacking the CXC chemokine PBSF/SDF-1. *Nature.* 1996;2:635–8.
9. Nagasawa T, Kikutani H, Kishimoto T. Molecular cloning and structure of a pre-B-cell growth-stimulating factor. *Proc Natl Acad Sci USA.* 1994;2:2305–9.
10. Aiuti A, Webb IJ, Bleul C, Springer T, Gutierrez-Ramos JC. The chemokine SDF-1 is a chemoattractant for human CD34+ hematopoietic progenitor cells and provides a new mechanism to explain the mobilization of CD34+ progenitors to peripheral blood. *J Exp Med.* 1997;2:111–20.
11. Zou YR, Kottmann AH, Kuroda M, Tanluchi I, Littman DR. Function of the chemokine receptor CXCR4 in hematopoiesis and in cerebellar development. *Nature.* 1998;2:595–9.
12. Tachibana K, Hirota S, Iizasa H, Yoshida H, Kawabata K, Kataoka Y, et al. The chemokine receptor CXCR4 is essential for vascularization of the gastrointestinal tract. *Nature.* 1998;2:591–4.
13. Feng Y, Broder CC, Kennedy PE, Berger EA. HIV-1 entry cofactor: functional cDNA cloning of a seven-transmembrane, G protein-coupled receptor. *Science.* 1996;2:872–7.
14. Doms RW, Peiper SC. Unwelcomed guests with master keys: how HIV uses chemokine receptors for cellular entry. *Virology.* 1997;2:179–90.
15. Sehgal A, Keener C, Boynton AL, Warrick J, Murphy GP. CXCR-4, a chemokine receptor, is overexpressed in and required for proliferation of glioblastoma tumor cells. *J Surg Oncol.* 1998;2:99–104.
16. Kijima T, Maulik G, Ma PC, Tibaldi EV, Turner RE, Rollins B, et al. Regulation of cellular proliferation, cytoskeletal function, and signal transduction through CXCR4 and c-Kit in small cell lung cancer cells. *Cancer Res.* 2002;2:6304–11.
17. Shibuta K, Begum NA, Mori M, Shimoda K, Akiyoshi T, Barnard GF. Reduced expression of the CXC chemokine hIRH/SDF-1 α mRNA in hepatoma and digestive tract cancer. *Int J Cancer.* 1997;2:656–62.
18. Muller A, Homey B, Soto H, Ge N, Catron D, Buchanan ME, et al. Involvement of chemokine receptors in breast cancer metastasis. *Nature.* 2001;2:50–56.
19. Koshiba T, Hosotani R, Miyamoto Y, Ida J, Tsuji S, Nakajima S, et al. Expression of stromal cell-derived factor 1 and CXCR4 ligand receptor system in pancreatic cancer: a possible role for tumor progression. *Clin Cancer Res.* 2000;2:3530–5.
20. Schols D, Struyf S, Van Damme J, Este JA, Henson G, De Clercq E. Inhibition of T-tropic HIV strains by selective antagonization of the chemokine receptor CXCR4. *J Exp Med.* 1997;2:1383–8.
21. Doranz BJ, Grovit-Ferbas K, Sharron MP, Mao SH, Goetz MB, Daar ES, et al. A small-molecule inhibitor directed against the chemokine receptor CXCR4 prevents its use as an HIV-1 coreceptor. *J Exp Med.* 1997;2:1395–1400.
22. Baba M, Nishimura O, Kanzaki N, Okamoto M, Sawada H, Iizawa Y, et al. A small-molecule, nonpeptide CCR5 antagonist with highly potent and selective anti-HIV-1 activity. *Proc Natl Acad Sci USA.* 1999;2:5698–703.
23. Dragic T, Trkola A, Thompson DA, Cormier EG, Kajumo FA, Maxwell E, et al. A binding pocket for a small molecule inhibitor of HIV-1 entry within the transmembrane helices of CCR5. *Proc Natl Acad Sci USA.* 2000;2:5639–44.

24. Murakami T, Nakajima T, Koyanagi Y, Tachibana K, Fujii N, Tamamura H, et al. A small molecule CXCR4 inhibitor that blocks T cell line-tropic HIV-1 infection. *J Exp Med*. 1997;2:1389-93.
25. Tamamura H, Omagari A, Hiramatsu K, Gotoh K, Kanamoto T, Xu Y, et al. Development of specific CXCR4 inhibitors possessing high selectivity indexes as well as complete stability in serum based on an anti-HIV peptide T140. *Bioorg Med Chem Lett*. 2001;2:1897-902.
26. Wada M, Doi R, Hosotani R, Lee JU, Fujimoto K, Koshihara T, et al. Expression of Bcl-2 and PCNA in duct cells after pancreatic duct ligation in rats. *Pancreas*. 1997;2:176-82.
27. Tamamura H, Xu Y, Hattori T, Zhang X, Arakaki R, Kanbara K, et al. A low-molecular-weight inhibitor against the chemokine receptor CXCR4: a strong anti-HIV peptide T140. *Biochem Biophys Res Commun*. 1998;2:877-82.
28. Scotton CJ, Wilson JL, Milliken D, Stamp G, Balkwill FR. Epithelial cancer cell migration: a role for chemokine receptors? *Cancer Res*. 2001;2:4961-5.
29. Robledo MM, Bartolome RA, Longo N, Rodriguez-Frade JM, Mellado M, Longo I, et al. Expression of functional chemokine receptors CXCR3 and CXCR4 on human melanoma cells. *J Biol Chem*. 2001;2:45098-105.
30. Mitra P, Shibuta K, Mathai J, Shimoda K, Banner BF, Mori M, et al. CXCR4 mRNA expression in colon, esophageal and gastric cancers and hepatitis C infected liver. *Int J Oncol*. 1999;2:917-25.
31. Helbig G, Christopherson KW 2nd, Bhat-Nakshatri P, Kumar S, Kishimoto H, Miller KD, et al. NF- κ B promotes breast cancer cell migration and metastasis by inducing the expression of the chemokine receptor CXCR4. *J Biol Chem*. 2003;2:21631-8.
32. Libura J, Drukala J, Majka M, Tomescu O, Navanot JM, Kucia M, et al. CXCR4-SDF-1 signaling is active in rhabdomyosarcoma cells and regulates locomotion, chemotaxis, and adhesion. *Blood*. 2002;2: 2597-606.
33. Riviere C, Subra F, Cohen-Solal K, Cordette-Lagarde V, Letestu R, Auclair C, et al. Phenotypic and functional evidence for the expression of CXCR4 receptor during megakaryocytopoiesis. *Blood*. 1999;2:1511-23.
34. Majka M, Janowska-Wieczorek A, Ratajczak J, Kowalska MA, Vilaire G, Pan ZK, et al. Stromal-derived factor 1 and thrombopoietin regulate distinct aspects of human megakaryopoiesis. *Blood*. 2000;2:4142-51.
35. Hodohara K, Fujii N, Yamamoto N, Kaushansky K. Stromal cell-derived factor-1 (SDF-1) acts together with thrombopoietin to enhance the development of megakaryocytic progenitor cells (CFU-MK). *Blood*. 2000;2:769-75.
36. Lataillade JJ, Clay D, Dupuy C, Rigal S, Jasmin C, Bourin P, et al. Chemokine SDF-1 enhances circulating CD34(+) cell proliferation in synergy with cytokines: possible role in progenitor survival. *Blood*. 2000;2:756-68.
37. Sehgal A, Ricks S, Boynton AL, Warrick J, Murphy GP. Molecular characterization of CXCR-4: a potential brain tumor-associated gene. *J Surg Oncol*. 1998;2:239-48.
38. Scotton CJ, Wilson JL, Scott K, Stamp G, Wilbanks GD, Fricker S, et al. Multiple actions of the chemokine CXCL12 on epithelial tumor cells in human ovarian cancer. *Cancer Res*. 2002;2:5930-8.
39. Taichman RS, Cooper C, Keller ET, Pienta KJ, Taichman NS, McCauley LK. Use of the stromal cell-derived factor-1/CXCR4 pathway in prostate cancer metastasis to bone. *Cancer Res*. 2002;2:1832-7.
40. Sanz-Rodriguez F, Hidalgo A, Teixido J. Chemokine stromal cell-derived factor-1 α modulates VLA-4 integrin-mediated multiple myeloma cell adhesion to CS-1/fibronectin and VCAM-1. *Blood*. 2001;2:346-51.
41. Ganju RK, Brubaker SA, Meyer J, Dutt P, Yang Y, Qin S, et al. The α -chemokine, stromal cell-derived factor-1 α , binds to the transmembrane G-protein-coupled CXCR-4 receptor and activates multiple signal transduction pathways. *J Biol Chem*. 1998;2:23169-75.

Indium-Mediated Atom-Transfer and Reductive Radical Cyclizations of Iodoalkynes: Synthesis and Biological Evaluation of HIV-Protease Inhibitors

Reiko Yanada,^{*,†} Yasuhiro Koh,[†] Nobuaki Nishimori,[†] Akira Matsumura,[†] Shingo Obika,[†] Hiroaki Mitsuya,^{*,‡} Nobutaka Fujii,[†] and Yoshiji Takemoto^{*,†}

Graduate School of Pharmaceutical Sciences, Kyoto University, Yoshida, Sakyo-ku, Kyoto 606-8501, Japan, Department of Internal Medicine II, Kumamoto University School of Medicine, Kumamoto, Japan, and Experimental Retrovirology Section, Medicine Branch, Division of Clinical Sciences, National Cancer Institute, National Institutes of Health, Bethesda, Maryland 20892

ryanada@pharm.kyoto-u.ac.jp; takemoto@pharm.kyoto-u.ac.jp

Received October 9, 2003

Novel indium-mediated radical cyclization reactions of aliphatic iodoalkynes have been studied. Treatment of iodoalkynes with a catalytic amount of In (0.1 equiv) and I₂ (0.05 equiv) promotes atom-transfer 5-exo cyclization to give five-membered alkenyl iodides. In contrast, reaction with In (2 equiv) and I₂ (1 equiv) yields reductive 5-exo cyclization products via the same 5-exo cyclization. Both processes are most likely initiated by low-valent indium species. To demonstrate versatility of these reactions, optically active HIV protease inhibitors were synthesized by this reductive cyclization method. Among them, several products, which contain a hydroxyethylamine dipeptide isostere as a transition state-mimicking substructure, proved to possess potent activity (IC₅₀ = 5–39 nM) against a wide spectrum of HIV strains, including multidrug-resistant variants.

Introduction

The use of radicals in organic synthesis has increased over the last two decades.¹ Tributyltin hydride has played an important role despite its neurotoxicity and the difficulty of complete removal of tin species from the reaction mixture.² Therefore, substantial efforts have been invested in the development of more convenient and useful reagents to replace tributyltin hydride.³ Indium (In)-mediated reactions have gained increasing popularity over the past decade as environmentally benign⁴ tools in organic synthesis.⁵ Since the first ionization potential of In is 5.8 eV, which is as low as those of Li and Na, it would be easy for In to promote SET (single-electron-transfer) processes. In addition, In is comparatively stable in air and, unlike many metals, has no apparent toxicity.⁶ We report herein the indium-mediated atom-transfer 5-exo cyclization (Kharasch-type reaction) and reductive 5-exo cyclization reaction of aliphatic iodoalkynes. In contrast to reductive radical cyclizations,^{3,4c} there are few reports on atom-transfer radical cyclizations.^{7,8}

We also have synthesized optically active furofuran P₂-ligands that are potent against a variety of HIV strains,

including multidrug-resistant variants, by combining optically active hexahydrofurofuran derivatives, synthesized using our indium-mediated reductive cyclization method, and substructural units of previously published HIV protease inhibitors.

(3) SmI₂: Curran, D. P.; Tottleben, M. J. *J. Am. Chem. Soc.* 1992, 114, 6050–6058. PhLi: Bailey, W. F.; Carson, M. W. *J. Org. Chem.* 1998, 63, 9960–9967. Et₂Zn: Vaupel, A.; Knochel, P. *J. Org. Chem.* 1998, 63, 5743–5753. Cobaloxime: Wakabayashi, K.; Yorimitsu, H.; Oshima, K. *J. Am. Chem. Soc.* 2001, 123, 5374–5375. Grignard reagent: Inoue, A.; Shinokubo, H.; Oshima, K. *Org. Lett.* 2000, 2, 651–653. Cp₂TiCl₂ + Grignard reagent: Nii, S.; Terao, J.; Kambe, N. *J. Org. Chem.* 2000, 65, 5291–5297. Cp₂TiCl: Gansäuer, A. *Synlett* 1998, 801–809. CrCl₂: Takai, K.; Matsukawa, N.; Takahashi, A.; Fujii, T. *Angew. Chem., Int. Ed.* 1998, 37, 152–155. Mn: Tang, J.; Shinokubo, H.; Oshima, K. *Tetrahedron* 1999, 55, 1893–1904. Et₃B + HGaCl₂: Mikami, S.; Fujita, K.; Nakamura, T.; Yorimitsu, H.; Shinokubo, H.; Matsubara, S.; Oshima, K. *Org. Lett.* 2001, 3, 1853–1855. Et₃B + Cp₂Zr(H)Cl: Fujita, K.; Nakamura, T.; Yorimitsu, H.; Oshima, K. *J. Am. Chem. Soc.* 2001, 123, 3137–3138. H₂PO₂: Yorimitsu, H.; Shinokubo, H.; Oshima, K. *Chem. Lett.* 2000, 104–105. Ph₄Si₂H₂ + Bu₃SnH: Yamazaki, O.; Yamaguchi, K.; Yokoyama, M.; Togo, H. *J. Org. Chem.* 2000, 65, 5440–5442. (TMS)₃SiH: Chatgillalloglu, C. *Acc. Chem. Res.* 1992, 25, 188–194. Cyclohexadienyl-silane: Studer, A.; Amrein, S. *Angew. Chem., Int. Ed.* 2000, 39, 3080–3082. Tri-2-furylgermane: Nakamura, T.; Yorimitsu, H.; Shinokubo, H.; Oshima, K. *Synlett* 1999, 1415–1416.

(4) (a) Li, C.-J. *Chem. Rev.* 1993, 93, 2023–2035. (b) Li, C.-J. *Tetrahedron* 1996, 52, 5643–5668. (c) Paquette, L. A. In *Green Chemistry: Frontiers in Benign Chemical Synthesis and Processing*; Anastas, P., Williamson, T., Eds.; Oxford University Press: New York, 1998.

(5) (a) Kang, S.; Jang, T.-S.; Keum, G.; Kang, S. B.; Han, S.-Y.; Kim, Y. *Org. Lett.* 2000, 2, 3615–3617. (b) Yanada, R.; Kaleda, A.; Takemoto, Y. *J. Org. Chem.* 2001, 66, 7516–7518 and references therein. (c) Inoue, K.; Sawada, A.; Shibata, I.; Baba, A. *J. Am. Chem. Soc.* 2002, 124, 906–907. (d) Miyabe, H.; Ueda, M.; Nishimura, A.; Naito, T. *Org. Lett.* 2002, 4, 131–134. (e) Miyabe, H.; Nishimura, A.; Ueda, M.; Naito, T. *Chem. Commun.* 2002, 1454–1455. (f) Tan, K. T.; Chng, S. S.; Cheng, H. S.; Loh, T. P. *J. Am. Chem. Soc.* 2003, 125, 2958–2963.

[†] Kyoto University.

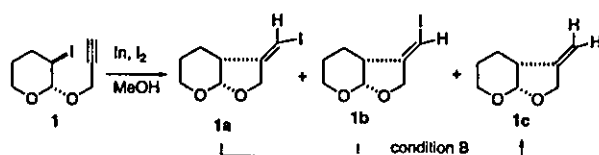
[‡] Kumamoto University School of Medicine.

^{*} National Institutes of Health.

(1) (a) Baguley, P. A.; Walton, J. C. *Angew. Chem., Int. Ed.* 1998, 37, 3072–3082. (b) Hirao, T. *Synlett* 1999, 175–181. (c) Yorimitsu, H.; Shinokubo, H.; Oshima, K. *Synlett* 2002, 674–686.

(2) (a) Curran, D. P.; Porter, N. A.; Giese, B. *Stereochemistry of Radical Reactions*; VCH Verlagsgesellschaft mbH: Weinheim, 1996. (b) Giese, B.; Kopping, B.; Göbel, T.; Dickhaut, J.; Thoma, G.; Kulicke, K. J.; Trach, F. *Organic Reactions*; John Wiley & Sons: New York, 1996; Vol. 48, pp 301–856.

TABLE 1. Radical Cyclization of Iodoalkyne 1*



run	condition	In (equiv)	I ₂ (equiv)	time (h)	yield (%)			total
					1a	1b	1c	
1		1	0.0	17	46	4	5	55
2	A	1	0.5	5	76	4	3	83
3		0.1	0.05	32	69	8	3	80
4	B	2	1.0	17	0	0	85	85

* Conditions A: 1 (2 mmol), In (2 mmol), I₂ (1 mmol), MeOH (4 mL). Conditions B: 1 (2 mmol), In (4 mmol), I₂ (2 mmol), MeOH (4 mL).

Atom-Transfer Cyclizations and Reductive Cyclizations of Iodoalkynes. We first investigated cyclization reactions of iodoalkyne 1 under various conditions. The results are summarized in Table 1. Iodoalkyne 1 was treated with In (1 equiv) in MeOH at room temperature to give 5-exo cyclized atom-transfer products 1a (*Z*) and 1b (*E*) in 50% yield (*Z*:*E* = 11.5:1, run 1). The *Z*-selectivity is in agreement with results reported by Curran et al.⁹ They analyzed the formation of (*Z*)- and (*E*)-vinyl iodides with the aid of a Curtin–Hammett kinetic scheme. In the case of compound 1, high stereoselectivity was observed and the *cis*-fused products 1a–c were obtained as shown by NMR spectroscopy (¹H–¹H NOESY and NOE spectra). *Trans*-fused products and 6-endo cyclization products were not observed. It is well-known that In reacts with I₂ in aromatic solvent under reflux to produce In¹⁺, In²⁺, and In³⁺.¹⁰ I₂ (0.5 equiv) was therefore added to In (1 equiv) in MeOH (condition A). The reaction proceeded smoothly to yield atom-transfer products 1a and 1b in 80% yield within 5 h (19:1, run 2). This atom-transfer-type reaction could be initiated by a catalytic amount of In and I₂. The reaction using In (0.1 equiv) and I₂ (0.05 equiv) gave the expected iodoolefins in 77% yield (1a:1b = 8.6:1, run 3), but the reaction took a long time.

Next, we used an excess amount of In. In (2 equiv) and I₂ (1 equiv) (condition B) gave only a reductive 5-exo cyclization product 1c in 85% yield (run 4). Compound 1c was also obtained from atom-transfer products 1a and

1b in 71% yield under condition B. Atom-transfer radical cyclization and reductive radical cyclization reactions were achieved for the first time by only controlling the quantities of In and I₂.

Next, we examined radical cyclizations to various aliphatic iodoalkynes (2–9) under conditions A and B. As can be seen from Table 2, iodoalkynes 2 and 4–6¹¹ predominantly gave atom-transfer cyclization products 2a, 4a, 5a, and 6a^{11,12} under conditions A and gave reductive cyclization products 2b, 4b,¹³ 5b,¹⁴ and 6b¹⁵ under conditions B (runs 1 and 3–5). Even under conditions A, the use of substrates 3 and 7 bearing an electron-delocalizing phenyl group on the sp carbon resulted in smooth reductive radical cyclization reactions to produce compounds 3b¹⁶ and 7b (runs 2 and 6). In general, it is thought that the reduction of vinyl radical intermediates (Scheme 1, D) to a vinyl-indium compound (E) is slower than the addition of iodine from compound 1 to give atom-transfer cyclization products (1a and 1b) under conditions A. On the other hand, vinylic radicals bearing phenyl groups (electrophilic radicals) might result in subsequent rapid electron transfer to produce a reductive radical cyclization product even under condition A. The atom-transfer cyclization or reductive cyclization may be realized by a subtle balance of reaction rates. We tried this reductive cyclization as an approach to synthesis of bicyclic sugars via radical cyclization (runs 7 and 8). Bicyclic sugars are interesting compounds because of their utility as building blocks for synthesis of natural products and because of their biological activities.¹⁷ The sugar iodides 8 and 9 were prepared from glucal and galactal with propargyl alcohol in the presence of *N*-iodosuccinimide in CH₃CN.¹⁸ Cyclization reactions with indium were carried out under conditions B using compounds 8 and 9.¹⁹ The reductive cyclization products 8b and 9b were obtained in 74 and 75% yields, respectively.

Intermolecular coupling reactions of alkyl iodide with electron-deficient olefins are well-known. To confirm the presence of radical intermediate D (Scheme 1), we investigated In-mediated cyclization of 1 in the presence of electron-deficient olefins such as α,β-unsaturated

(11) Haaïma, G.; Hanton, L. R.; Lynch, M.-J.; Mawson, S. D.; Routledge, A.; Weavers, R. T. *Tetrahedron* 1994, 50, 2161–2174.

(12) Haaïma, G.; Lynch, M.-J.; Routledge, A.; Weavers, R. T. *Tetrahedron* 1993, 49, 4229–4252.

(13) Okuma, K.; Kamahori, Y.; Tsubakihara, K.; Yoshihara, K.; Tanaka, Y.; Shioji, K. *J. Org. Chem.* 2002, 67, 7355–7360.

(14) Trost, B. M.; Marrs, C. M. *J. Am. Chem. Soc.* 1993, 115, 6636–6645.

(15) Haaïma, G.; Lynch, M.-J.; Routledge, A.; Weavers, R. T. *Tetrahedron* 1991, 47, 5203–5214.

(16) Torii, S.; Inokuchi, T.; Yukawa, T. *J. Org. Chem.* 1985, 50, 5875–5877.

(17) Recently, bicyclic sugars have been prepared extensively with Bu₃SnH. (a) Ferrier, R. J.; Petersen, P. M. *Tetrahedron* 1990, 46, 1–11. (b) De Mesmaeker, A.; Hoffman, P.; Winkler, T.; Waldner, *Synlett* 1990, 201–204. (c) Moufid, N.; Chapleur, Y.; Mayon, P. *J. Chem. Soc., Perkin Trans. 1* 1992, 991–998. (d) Lesueur, C.; Nouguler, R.; Bertrand, M. P.; Hoffmann, P.; De Mesmaeker, *Tetrahedron* 1994, 50, 5369–5380. (e) Mayer, S.; Prandi, J.; Bamhaoud, T.; Bakkas, S.; Guillou, O. *Tetrahedron* 1998, 54, 8753–8770. (f) Yamazaki, O.; Yamaguchi, K.; Yokoyama, M.; Togo, H. *J. Org. Chem.* 2000, 65, 5440–5442.

(18) α-Isomers 8 and 9 were obtained predominantly (8: 75% yield, α:β = 13:1; 9: 74% yield, α:β = 14:1). (a) Audin, C.; Lancelin, J.-M.; Beau, J.-M. *Tetrahedron Lett.* 1988, 29, 3691–3694. (b) De Mesmaeker, A.; Hoffmann, P.; Ernst, B. *Tetrahedron Lett.* 1989, 30, 57–60.

(19) Cyclization products 8b and 9b were probably deacetylated by InX₃(OMe)₃. Thus, reacylation with acetic anhydride and (dimethylamino)pyridine in THF was done.

(6) (a) Nakajima, M.; Takahashi, H.; Sasaki, M.; Kobayashi, Y.; Ohno, Y.; Usami, M. *Teratog., Carcinog., Mutagen.* 2000, 20, 219–227. (b) Nakajima, M.; Sasaki, M.; Kobayashi, Y.; Ohno, Y.; Usami, M. *Teratog., Carcinog., Mutagen.* 1999, 19, 205–209.

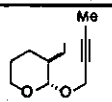
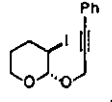
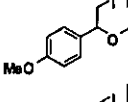
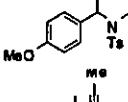
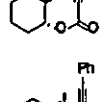
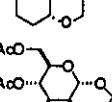
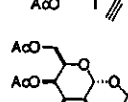
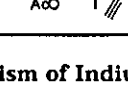
(7) (a) Yorimitsu, H.; Nakamura, T.; Shinokubo, H.; Oshima, K. *J. Org. Chem.* 1998, 63, 8604–8605. (b) Chakraborty, A.; Marek, I. *Chem. Commun.* 1999, 2375–2376. (c) Yorimitsu, H.; Nakamura, T.; Shinokubo, H.; Oshima, K.; Omoto, K.; Fujimoto, H. *J. Am. Chem. Soc.* 2000, 122, 11041–11047.

(8) Atom-transfer cyclization reactions with Bu₃SnH have been reported. (a) Curran, D. P.; Chen, M.-H.; Kim, D. *J. Am. Chem. Soc.* 1986, 108, 2489–2490. (b) Curran, D. P.; Chen, M.-H.; Kim, D. *J. Am. Chem. Soc.* 1989, 111, 6265–6276.

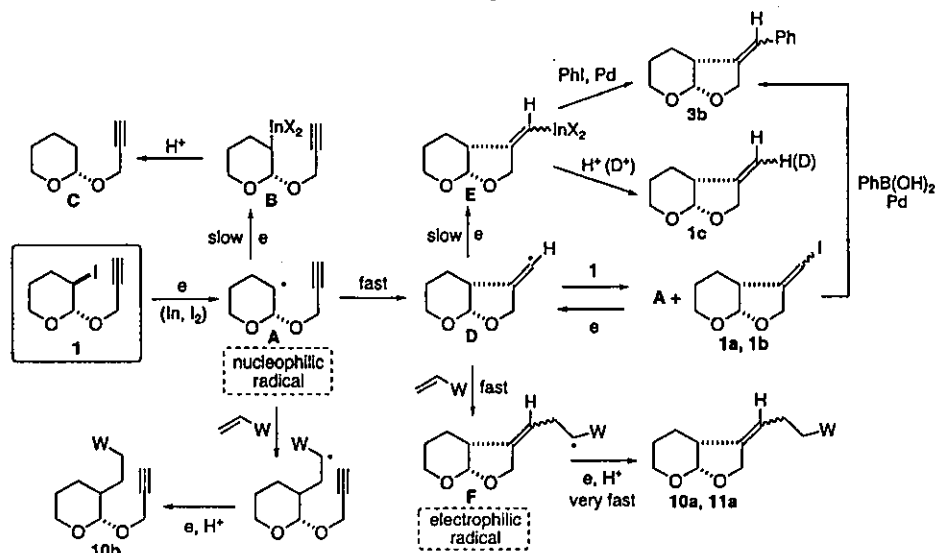
(9) Curran, D. P.; Chen, M.-H.; Kim, D. *J. Am. Chem. Soc.* 1989, 111, 6265–6276.

(10) (a) Freeland, B. H.; Tuck, D. G. *Inorg. Chem.* 1976, 15, 475–476. In reacts with I₂ in a refluxing aromatic solvent to form InI₃. A solution of InI₃ reacts with excess In under reflux with gradual precipitation of pure, highly crystalline InI₂. On treatment of InI₂ with diethyl ether or other Lewis bases, the insoluble InI₂ is precipitated and the corresponding InI₃–Lewis base adduct is formed. (b) Marshall, J. A.; Grant, C. M. *J. Org. Chem.* 1999, 64, 8214–8219.

TABLE 2. Radical Cyclizations of Various Iodoalkynes 2–9

Run	Substrate	Time (h)	Condition	Solvent	Product	Yield (%) (E/Z ratio)	
						Atom-transfer a	Reductive b
1		5	A	MeOH	2a	60	0
		5	B	MeOH	2b	(1 : 3.6)	65 (1 : 1)
2		8	A	MeOH	3b	0	73 (8.1 : 1)
3		18	A	MeOH	4a	67	0
		48	B	DMF	4b	(1 : 1.3)	86
4		18	A	MeOH	5a	70	8
		48	B	DMF	5b	(1 : 1.5)	82
5		24	A	DMF	6a	41	0
		48	B	DMF	6b	(1 : 3.4)	21 (1.3 : 1)
6		30	A	MeOH	7b	0	57 (2 : 1)
7		20	B	DMF	8b	0	74
8		20	B	DMF	9b	0	75

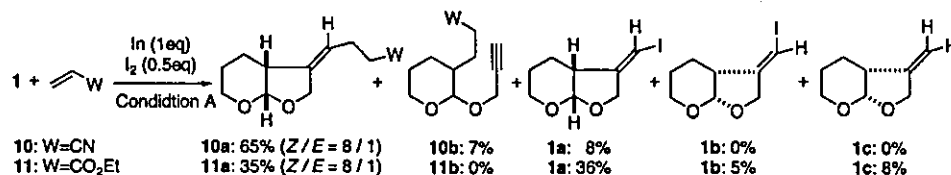
SCHEME 1. Mechanism of Indium-Mediated Radical Cyclization Reaction



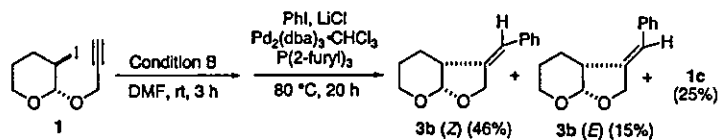
nitrile and ester in a protic solvent, MeOH (Scheme 2). When **1** was subjected to conditions A with acrylonitrile or ethyl acrylate (2 equiv), the desired compounds **10a** or **11a** were obtained in 65 and 35% yields, respectively, with or without compounds **10b**, **1a**, **1b**, and **1c**.

Furthermore, we carried out palladium-catalyzed cross-coupling reaction (Oshima's reaction)²¹ in order to confirm that vinyl indium intermediate **E** is generated from compound **1** (Scheme 3). After treatment of compound **1** under conditions B in DMF, iodobenzene (0.9 equiv),

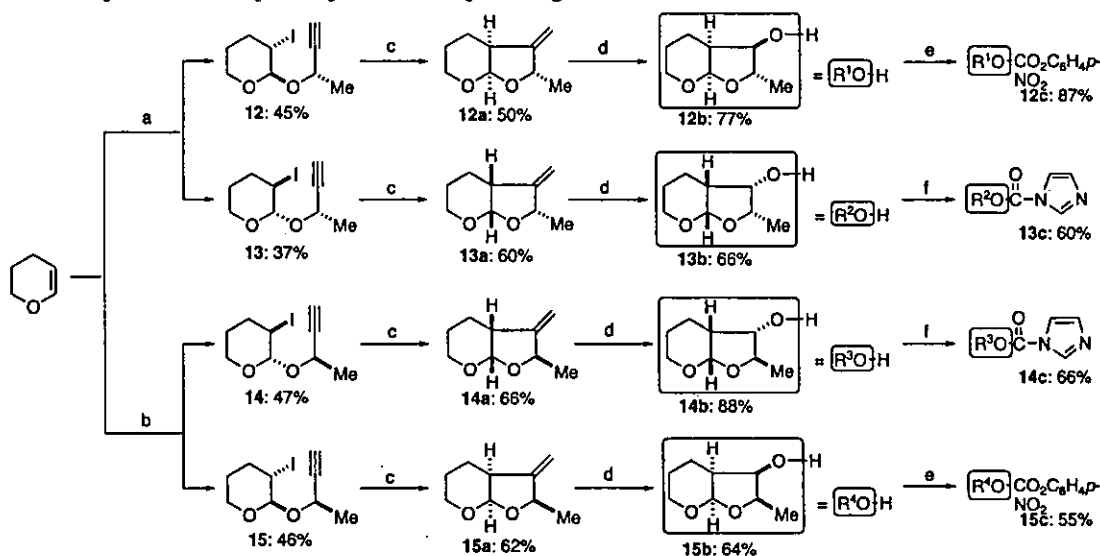
SCHEME 2. Intermolecular 1,4-Addition to Electron-Deficient Olefins



SCHEME 3. Application to Oshima's Reaction



SCHEME 4. Synthesis of Optically Active Bicyclic Ligands*



* Conditions: (a) *N*-Iodosuccinimide, (*S*)-(-)-3-butyn-2-ol, CH₂Cl₂, 0 °C-rt. (b) *N*-Iodosuccinimide, (*R*)-(+)-3-butyn-2-ol, CH₂Cl₂, 0 °C-rt. (c) In, I₂, MeOH, rt. (d) (1) O₃, MeOH, rt; (2) NaBH₄, rt. (e) 4-Nitrophenyl chloroformate, Et₃N, CH₂Cl₂, rt. (f) 1,1'-Carbonyldiimidazole, KOH (cat), toluene.

palladium-trifurylphosphine complex, prepared from Pd₂(dba)₃·CHCl₃ (0.02 equiv) and trifurylphosphine (0.12 equiv) in THF, and lithium chloride²² (3 equiv) were added to the reaction mixture. Then, the reaction mixture was heated at 80 °C for 20 h to provide the corresponding coupling products **3b** in 61% yield (*Z*:*E* = 3:1) accompanied with the reductive cyclization product **1c** (25% yield). The geometrical chemistry of compounds **3b** (*Z* and *E*) was determined by NOE experiments of ¹H NMR. The results showed the presence of vinyl indium intermediate **E**.

On the basis of the above-described results, we propose the following reaction mechanism (Scheme 1). Treatment

of compound **1** with low-valent indium (In, In⁺, and/or In²⁺), produced by In and I₂ in MeOH, provides alkyl radical **A** (nucleophilic radical). In general, it is not easy for radical **A** to be reduced to compound **C** through alkyl indium intermediate **B**.²³ Alkyl radical **A** smoothly undergoes a radical cyclization reaction to produce vinyl radical **D**. This radical is readily reduced to vinyl indium compound **E**²⁴ when there are enough low-valent indium species. Protonation of **E** produces **1c**, whereas the Oshima reaction of **E** produces **3b**. When there is only a small amount of reducing agent, radical **D** abstracts the iodine radical from compound **1** to produce vinyl iodides **1a** and **1b** and to reproduce alkyl radical **A**. In the presence of α,β -unsaturated compounds, intermolecular addition of radical **D** to the activated olefins occurred to give radical **F** (electrophilic radical). Sequential addition of one electron and one proton proceeded smoothly to give

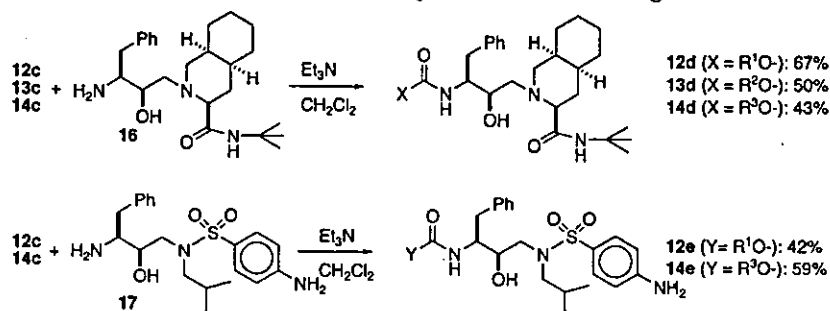
(20) (a) Shono, T.; Nishiguchi, I.; Sasaki, M. *J. Am. Chem. Soc.* **1978**, *100*, 4314–4315. (b) Luche, J. L.; Allavena, C. *Tetrahedron Lett.* **1988**, *29*, 5369–5372. (c) Blanchard, P.; Da Silva, A. D.; El Kortbi, M. S.; Fourrey, J.-L.; Robert-Géro, M. *J. Org. Chem.* **1993**, *58*, 6517–6519. (d) Takai, K.; Ueda, T.; Ikeda, N.; Moriwake, T. *J. Org. Chem.* **1996**, *61*, 7990–7991.

(21) Takaki, K.; Yorimitsu, H.; Shinokubo, H.; Matsubara, S.; Oshima, K. *Org. Lett.* **2001**, *3*, 1997–1999.

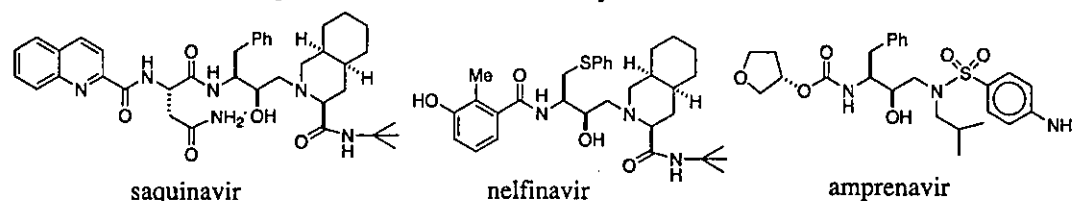
(22) Hirashita, T.; Hayashi, Y.; Mitsui, K.; Araki, S. *J. Org. Chem.* **2003**, *68*, 1309–1313.

(23) (a) Nugent, W. A.; RajanBabu, T. V. *J. Am. Chem. Soc.* **1988**, *110*, 8561–8562. (b) Curran, D. P.; Fevig, T. L.; Tottleben, M. J. *Synlett* **1990**, 773–774.

(24) Quenching with DCI in MeOD under Conditions B yielded the deuterated compound **1c** (89% D, *Z*:*E* = 19:1).

SCHEME 5. Synthesis of Various Inhibitors with Bicyclic Ethers as P₂ Ligands

SCHEME 6. Structures of Saquinavir, Nelfinavir, and Amprenavir



heterocyclic compounds **10a** and **11a** in moderate yields. The reduction of an alkenyl radical **D** to an alkenyl indium compound **E** is slower than 1,4-addition of the radical **D** to α,β -unsaturated compounds. However, one-electron transfer to the resulting radical **F** having electron-withdrawing groups proceeds faster than addition to a different unsaturated bond.

Synthesis of Optically Active HIV Protease Inhibitors and Biological Evaluation. Ghosh et al.²⁵ reported that stereochemically defined hexahydrofuro-pyrans play a crucial role as the replacement of asparagine side chain of Ro 31-8959-based HIV protease inhibitors.²⁶ They also reported that a fused bicyclic ligand with oxygens properly positioned could effectively form a hydrogen bond to the NH of Asp 29 and 30 residues corresponding to the quinardic amide-asparagine amide fragment of the Ro 31-8959 inhibitor.²⁷

We applied the indium-mediated reductive cyclization to the synthesis of optically active hexahydrofuro-pyrans derivatives as HIV protease inhibitors with novel P₂-pharmacophores (Schemes 4 and 5). As shown in Scheme 4, the reaction of dihydropyran with *N*-iodosuccinimide and (*S*)- or (*R*)-3-butyn-2-ol gave optically active iodo ethers **12**–**15** in good yields. Radical cyclizations of **12**–**15** with In and I₂ under conditions B afforded the bicyclic acetals **12a**–**15a** (50–66%). Ozonolytic cleavage followed

(25) Ghosh, A. K.; Kincaid, J. F.; Walters, D. E.; Chen, Y.; Chaudhuri, N. C.; Thompson, W. J.; Culbertson, C.; Fitzgerald, P. M. D.; Lee, H. Y.; McKee, S. P.; Munson, P. M.; Duong, T. T.; Darke, P. L.; Zugay, J. A.; Schleif, W. A.; Axe, M. G.; Lin, J.; Huff, J. R. *J. Med. Chem.* 1996, 39, 3278–3290.

(26) Roberts, N. A.; Martin, J. A.; Kinchington, D.; Broadhurst, A. V.; Craig, J. C.; Duncan, I. B.; Galpin, S. A.; Handa, B. K.; Kay, J.; Krohn, A.; Lambert, R. W.; Merrett, J. H.; Mills, J. S.; Parkes, K. E. B.; Redshaw, S.; Ritchie, A. J.; Taylor, D. L.; Thomas, G. J.; Machin, P. J. *Science* 1990, 248, 358–361.

(27) (a) Ghosh, A. K.; Thompson, W. J.; Holloway, M. K.; McKee, S. P.; Duong, T. T.; Lee, H. Y.; Munson, P. M.; Smith, A. M.; Wai, J. M.; Darke, P. L.; Zugay, J. A.; Emint, E. A.; Schleif, W. A.; Huff, J. R.; Anderson, P. S. *J. Med. Chem.* 1993, 36, 2300–2310. (b) Thompson, W. J.; Ghosh, A. K.; Holloway, M. K.; Lee, H. Y.; Munson, P. M.; Schwering, J. E.; Wai, J. M.; Darke, P. L.; Zugay, J. A.; Emint, E. A.; Schleif, W. A.; Huff, J. R.; Anderson, P. S. *J. Am. Chem. Soc.* 1993, 115, 801–803.

TABLE 3. Anti-HIV Activities, Cytotoxicities, and HIV Protease Inhibitory Activities of the Synthetic Compounds

run	compd	IC ₅₀ (nM) ^a	CC ₅₀ (μM) ^b	SI ^c
1	12d	39 ± 15	36.4 ± 3.5	930
2	13d	6 ± 2	32.9 ± 3.3	5480
3	14d	5 ± 3	27.8 ± 2.1	5560
4	12e	26 ± 4	30.3 ± 4.9	1170
5	14e	30 ± 10	40.0 ± 5.2	1330
6	saquinavir	17 ± 3	11 ± 3	650
7	amprenavir	36 ± 11	>100	>2780

^a IC₅₀ values are based on the inhibition of HIV-induced cytopathogenicity in MT-2 cells. ^b CC₅₀ values are based on the reduction of the viability of mock-infected MT-2 cells (±1 standard deviation). All values represent the means from at least three independent experiments. ^c Selectivity index (SI) is shown as CC₅₀/IC₅₀.

by the reduction of the resulting ketones with sodium borohydride in methanol at –78 °C furnished stereoselectively the optically active endo alcohols **12b**–**15b** in 64–88% yields. The stereochemical assignments of these alcohols **12b**–**15b** were determined by NOE experiments of ¹H NMR. The reaction of hexahydrofuro-pyran ligands **12b** and **15b** with 4-nitrophenyl chloroformate and triethylamine in methylene chloride afforded the active carbonates **12c** and **15c** in good yields. The compounds **13c** and **14c** could not be obtained by the same reaction. We therefore used 1,1'-carbonyldiimidazole instead of 4-nitrophenyl chloroformate. The ligands **13b** and **14b** with 1,1'-carbonyldiimidazole and potassium hydroxide in toluene afforded the active carbonates **13c** and **14c** in good yields.

Novel optically active hydroxyethylamine isosteres **12d**–**14d** bearing decahydroisoquinoline unit **16**^{28,29} and **12e** and **14e** bearing sulfonamide unit **17**³⁰ were synthesized according to Ghosh's methods³¹ (42–67% yields).

(28) Roberts, N. A.; Martin, J. A.; Kinchington, D.; Broadhurst, A. V.; Craig, J. C.; Duncan, I. B.; Galpin, S. A.; Handa, B. K.; Kay, J.; Krohn, A.; Lambert, R. W.; Merrett, J. H.; Mills, J. S.; Parkes, K. E. B.; Redshaw, S.; Ritchie, A. J.; Taylor, D. L.; Thomas, G. J.; Machin, P. J. *Science* 1990, 248, 358–361.